2006). In this study, we investigated whether two major female sex hormones, E2 and Prog, play a functional role in HILI.

2. Materials and methods

2.1. Materials

HAL was purchased from Takeda (Osaka, Japan) and isoflurane (Iso) was from Abott Japan (Tokyo, Japan). 17β-Estradiol (E2) and Prog were from Sigma–Aldrich (St. Louis, MO). ICI182,780 (ICI) was from TOCRIS bioscience (Ellisville, MO) and RU486 (RU) was from Tokyo Kasei (Tokyo, Japan). Rabbit polyclonal antibody against myeloperoxidase (MPO) was from DAKO (Carpinteria, CA). All primers were commercially synthesized at Hokkaido System Sciences (Sapporo, Japan). All other chemicals were of the highest grade commercially available.

2.2. Mice and HAL-administration

Female BALB/cCrSlc mice (8 weeks old, 18–21 g) were obtained from SLC Japan (Hamamatsu, Japan). Animals were housed in a controlled environment (temperature 25 ± 1 °C, humidity 50 ± 10%, and 12-h light/12-h dark cycle) in the institutional animal facility with access to food and water *ad libitum*. Animals were acclimatized before use for the experiments (Sugaya et al., 2000). E2 and Prog pretreatment methods were modified from those of a previous report that the serum hormone levels were almost the same or slightly higher than those during late pregnancy in rodent, although the mice used in the present study were not ovariectomized since we intend to perform the present studies under the autologus condition and to mimic the condition of late pregnancy. Mice were pretreated with E2 (0.3 μg/mouse, *s.c.*) or Prog (0.3 mg/mouse, *s.c.*) for 7 days followed by HAL administration (15 or 30 mmol/kg, dissolved in olive oil 2 mL/20 g of body weight, *i.p.*) 1.5 h after the last E2 or Prog treatment. Mice were pretreated with the receptor antagonist, ICI (Estrogen receptor (ER) antagonist, 50 μg/mouse, *s.c.*) or RU (Progesterone receptor (PR) antagonist, 50 μg/mouse, *s.c.*) 0.5 h before the E2 or Prog treatment, respectively. In the Isoflurane (Iso) administration experiment, Iso was administered instead of HAL. Mice were sacrificed and the plasma and the liver were collected 3, 6 and 24 h after the HAL administration. The liver was fixed in buffered neutral 10% formalin and used for immunohistochemical staining. The degree of liver injury was assessed by hematoxylin–eosin (H&E) staining and the plasma aspartate aminotransferase (AST) and alanine aminotransferase (ALT) levels were determined using Fuji Dri-Chem 4000V (Fuji Film Med. Co., Tokyo, Japan). The neutrophil infiltration was assessed by immunostaining for MPO as previously described (Kumada et al., 2004). Animal maintenance and treatment were conducted in accordance with the National Institutes of Health Guide for Animal Care and Use Committee of Kanazawa University, Japan.

2.3. Measurement of plasma E2, Prog and IL-17 levels

Plasma E2 and Prog were measured by enzyme immunoassay (EIA) using Estradiol-17β (serum/plasma) EIA kit and Progesterone EIA kit from Assay Designs Inc. (Ann Arbor, MI) according to the manufacturer's instructions. The plasma IL-17 level was measured by ELISA using a Ready-SET-GO! Mouse Interleukin-17A (IL-17A) kit from eBioscience (San Diego, CA) according to the manufacturer's instructions.

2.4. Immunoblot analysis

SDS-polyacrylamide gel electrophoresis and immunoblot analysis were perfomed. Mouse liver homogenates (30 μg) were separated on 10% polyacrylamide gels and electrotransferred onto polyvinylidene difluoride membrane, Immobion-P (Millipore Corporation, Billerica, MA). The membranes were probed with goat anti-rat Cyp2e1 (1:10,000, Daiichi Pure Chemicals, Tokyo, Japan), anti-TFA antisera (1:1000, kindly provided by Dr. Lance Pohl, National Institutes of Health, Bethesda, MD) and rabbit anti-human glyceraldehyde-3-phoshate dehydrogenase (GAPDH) polyclonal antibodies (1:100, IMAGENEX, San Diego, CA) and the corresponding fluorescent dye-conjugated second antibody (1:5000) and an Odyssey Infrared Imaging System (LI-COR Biosciences, Lincoln, NE) were used for detection. The relative expression level was quantified using ImageQuant TL Image Analysis software (GE Healthcare, Buckinghamshire, UK).

2.5. Glutathione assay

Mouse liver was homogenized with a glass homogenizer on ice-cold 5% sulfosalicylic acid and centrifuged at 8000 × *g* at 4 °C for 10 min. Total GSH and GSSG concentration in the supernant were measured as described previously (Tietze, 1969; Griffith, 1980). GSH was calculated from the difference between the total GSH and GSSG concentration.

Table 1
Sequence of primers used for real-time RT-PCR analyses in this study.

Target	Primer	Sequence
TNFα	FP	5′-TGT CTC AGC CTC TTC TCA TTC C-3′
	RP	5′-TGA GGG TCT GGG CCA TAG AAC-3′
IL-1β	FP	5′-GTT GAC GGA CCC CAA AAG AT-3′
	RP	5′-CAC ACA CCA GCA GGT TAT CA-3′
IL-6	FP	5′-CCA TAG CTA CCT GGA GTA CA-3′
	RP	5′-GGA AAT TGG GGT AGG AAG GA-3′
CXCL1	FP	5′-GAT TCA CCT CAA GAA CAT CCA GAG-3′
	RP	5′-GAA GCC AGC GTT CAC CAG AC-3′
CXCL2	FP	5′-AAG TTT GCC TTG ACC CTG AAG-3′
	RP	5′-ATC AGG TAC GAT CCA GGC TTC-3′
ICAM-1	FP	5′-CAA GGA GAT CAC ATT CAC GG-3′
	RP	5′-CTT CCA GGG AGC AAA ACA AC -3′

FP, forward primer; RP, reverse primer.

2.6. Protein carbonyl content measurement

The protein carbonyl was measured in whole liver homogenate using a Protein Carbonyl kit (Cell biolabs, Tokyo, Japan). The assay was performed according to the manufacturer's instructions.

2.7. Real-time reverse transcription (RT)-PCR analysis

RNA from mouse liver was isolated using RNAiso according to the manufacturer's instructions. Tumor necrosis factor α (TNFα), Interleukin (IL)-1β, IL-6, Chemokine (C-X-C motif) ligand 1, 2 (CXCL1, CXCL2), intercellular adhesion molecule-1 (ICAM-1), and Gapdh were quantified by real-time RT-PCR. The primer sequences used in this study are shown in Table 1. The reverse transcription process and real-time RT-PCR were performed as described previously (Kobayashi et al., 2009).

2.8. Statistical analysis

Data are presented as mean ± SD. Comparison of 2 groups was made with an unpaired, two-tailed Student's *t*-test. Comparison of multiple groups was made with ANOVA followed by Dunnett or Tukey test. A value of $P < 0.05$ was considered statistically significant.

3. Results

3.1. The effects of E2 and Prog on halothane-induced liver injury

To investigate the role of the female sex hormones on HILI, female BALB/c mice pretreated with E2 or Prog were administered with HAL at a dose of 30 or 15 mmol/kg, respectively. The plasma E2 levels were 87.72 ± 15.98 pg/mL in mice 24 h after the last E2 pretreatment and 42.39 ± 18.85 pg/mL in mice pretreated with vehicle. The plasma Prog levels was 80.43 ± 33.25 ng/mL in mice 24 h after the last Prog pretreatment and 29.24 ± 14.77 ng/mL in mice pretreated with vehicle. Plasma transaminase levels were not changed 3 and 6 h after the HAL administration (data not shown). In addition, E2 or Prog pretreatment only did not affect the plasma transaminase levels 3 and 6 h after the HAL administration (data not shown). At 24 h after the HAL administration, E2 pretreatment significantly decreased the plasma transaminase levels compared with HAL (30 mg/kg) alone and Prog pretreatment caused a remarkable increase of the plasma transaminase levels compared to HAL (15 mg/kg) alone. These effects were significantly inhibited by pretreatment with ICI (ER antagonist) or RU (PR antagonist) in E2 or Prog pretreated groups, respectively (Fig. 1A). Histopathological changes demonstrated that E2 pretreatment decreased hepatocyte degeneration and damage lesions, which were enhanced by Prog pretreatment. In addition, immunohistochemical analyses with anti-MPO antibody demonstrated that E2 pretreatment decreased the numbers of MPO-positive cells infiltrated in liver at 24 h after HAL administration, whereas Prog pretreatment increased (Fig. 1B). From these results, pretreatment of mice with E2 attenuated HILI, whereas pretreatment of mice with Prog exacerbated HILI and these effects were likely mediated via each hormone receptor. Iso,

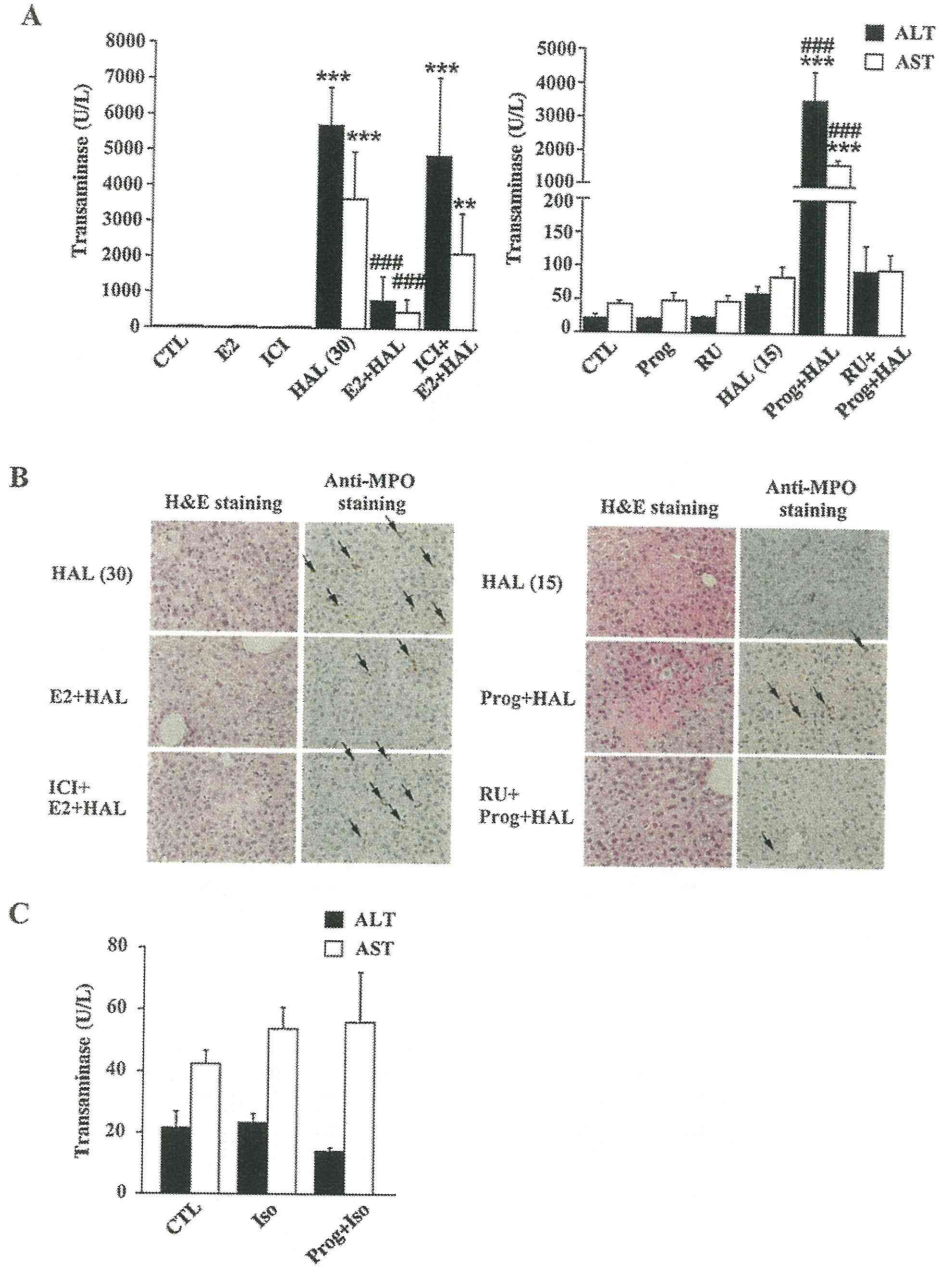

Fig. 1. Effects of E2 or Prog administration in HAL-induced liver injury. Mice (female, 8-week old) were pretreated with E2 (0.3 μg/mouse, *s.c.*), Prog (0.3 mg/mouse, *s.c.*) or vehicle (CTL: olive oil) for 7 days followed by HAL administration (15 or 30 mmol/kg, *i.p.*) or Iso administration (15 mmol/kg, *i.p.*) 1.5 h after the last treatment of E2 or Prog. In experiments using antagonist, mice were treated with ICI (50 μg/mouse, *s.c.*) or RU (50 μg/mouse, *s.c.*) 0.5 h prior to the treatment with E2 or Prog, respectively for 7 days. Twenty-four hours after the HAL or Iso administration, serum samples were collected for assessment of the transaminase levels (A and C). Liver tissue sections were stained with H&E or immunostained with anti-MPO antibody (B). Arrows indicate MPO-positive cells. The data are mean ± SD of 4–5 mice. $^{**}P < 0.01$ and $^{***}P < 0.001$, compared with CTL. $^{###}P < 0.001$, compared with only HAL-administered mice.

structurally and pharmacologically similar to HAL, is less hepatotoxic than HAL (Njoku et al., 1997). In female BALB/c mice, the transaminase levels were not increased at doses up to 30 mmol/kg of Iso (data not shown). In addition, Prog pretreatment showed no effects on the serum transaminase levels at 24 h after the Iso administration (Fig. 1C).

3.2. E2 and Prog had no effect on the metabolic activation of halothane or on the oxidative stress

HAL is metabolized by CYP2E1 to reactive metabolites, trifluoroacetyl radicals, which bind a number of hepatic proteins in human, rats and mice (Bourdi et al., 2001; Njoku et al., 1997; Gut et al., 1993). To investigate whether the pretreatment with E2 or Prog affected the metabolic activation of HAL, immunoblotting was performed using anti-TFA polyclonal antibody and goat anti rat Cyp2e1 antibody. No difference was found in either the profiles or levels of TFA–protein adducts formed in the liver of mice pretreated with E2 or Prog 24 h after the HAL administration (Fig. 2A). In addition, the expression levels of Cyp2e1 protein in E2- or Prog-pretreated mouse liver also showed no changes (Fig. 2B). GSH plays a protective role against HILI in guinea pig (Lind et al., 1992). To investigate whether GSH and oxidative stress were modulated by pretreatment with E2 or Prog, the ratio of GSH/GSSG and

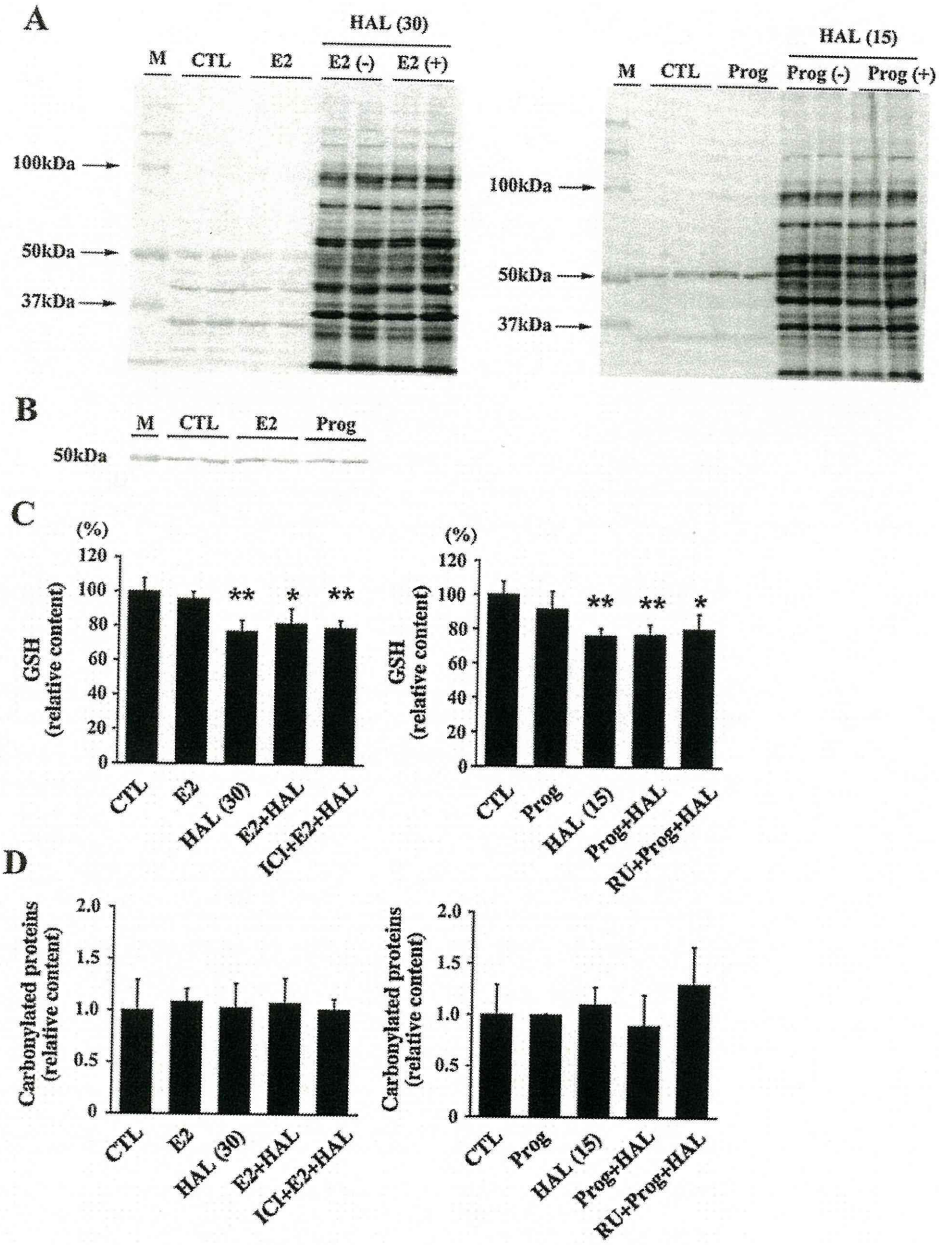

Fig. 2. Effects of E2 or Prog administration on the degree of metabolic activation, the ratio of GSH/GSSG and oxidative stress in the liver in HAL-induced liver injury. Experimental conditions for animal treatments were the same as those in Fig. 1. Twenty-four hours after the HAL administration, liver samples were collected. Immunoblot of TFA–protein adducts (A), Cyp2e1 protein expression (B) and Gapdh, a lording control, were performed using whole liver homogenate. Each lane shows an individual mouse (30 μg/lane). The ratio of GSH/GSSG (C) and carbonylated proteins (D) in whole liver homogenate were measured. The data are mean ± SD of 4 mice. $^{*}P < 0.05$ and $^{**}P < 0.01$, campared with CTL. M: molecular weight marker.

carbonylated proteins, a biomarker of oxidative stress, in the liver were measured. The ratio of GSH/GSSG of the HAL-administered groups were significantly decreased to 50–70% of the control group, but there was no effect on the ratio of GSH/GSSG in E2- or Prog-pretreated mouse liver (Fig. 2C). In addition, the levels of carbonylated proteins were also not altered (Fig. 2D). These results indicated that E2 and Prog had no effect on the metabolic activation of HAL or on the oxidative stress.

3.3. E2 and Prog modulated the immune responses in halothane-induced liver injury

In many cases, inflammation reactions and immune-related cells play a crucial role in DILI. In HILI, proinflammatory cytokines and neutrophils play important roles in the propagation of tissue damage (You et al., 2006; Kobayashi et al., 2009; Cheng et al., 2010). To investigate whether E2 or Prog pretreatment affect the production of inflammatory cytokines (TNFα, IL-1β and IL-6), potent neutrophil chemotactic chemokines, CXCL1 and CXCL2, and ICAM-1, which are important in the transendothelial migration of neutrophils, hepatic mRNA was measured. E2 pretreatment alone did not affect the production of proinflammatory cytokines, chemokines and ICAM-1 (Fig. 3). The expression of TNFα, IL-1β and IL-6 were significantly increased compared with CTL at indicated time after the HAL administration (Fig. 3A). Similarly, CXCL1 and ICAM-1 were significantly increased compared with CTL at 3 and 6 h after HAL administration and CXCL2 was markedly increased at 24 h after the HAL administration (Fig. 3B). Moreover, E2 pretreat-

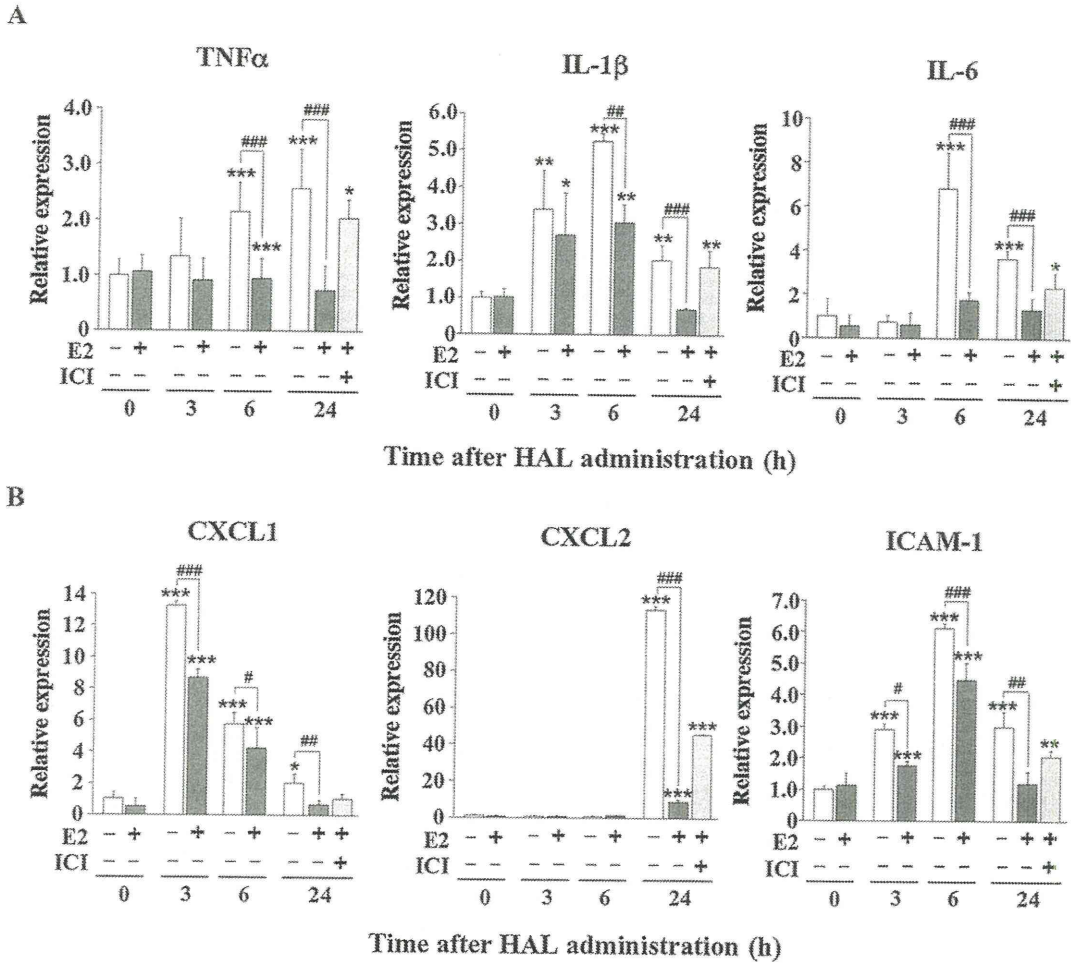

Fig. 3. Time-dependent changes of immune responses by E2 pretreatment in HAL-administered mice. Experimental conditions for animal treatments were the same as those in Fig. 1. Relative expression of hepatic mRNA was measured for proinflammatory cytokines (A) and chemokines and ICAM-1 related to neutrophil infiltration (B) in the E2-pretreated mouse liver 0, 3, 6 and 24 h after the HAL administration. Expression of hepatic mRNA was normalized to Gapdh mRNA. The data are mean ± SD of 4–5 mice. $^{*}P<0.05$, $^{**}P<0.01$ and $^{***}P<0.001$, campared with CTL. $^{\#}P<0.05$, $^{\#\#}P<0.01$ and $^{\#\#\#}P<0.001$, compared with only HAL-administered mice.

ment significantly decreased inflammatory mediators compared with HAL alone. These effects of E2 were blocked by ICI administration (Fig. 3).

Interestingly, Prog pretreatment alone significantly upregulated CXCL1, whereas proinflammatory cytokines, CXCL2 and ICAM-1 did not change (Fig. 4). Prog pretreatment significantly increased the expression of TNFα, IL-1β and IL-6 at indicated time after the HAL administration (Fig. 4A). Similarly, Prog pretreatment significantly increased CXCL1, CXCL2 and ICAM-1 at indicated time after the HAL administration (Fig. 4B). These effects of Prog were blocked by RU administration (Fig. 4). These results suggested that E2 and Prog played a crucial role in HILI by modulating the hepatic inflammation.

3.4. E2 and Prog modulated the production of IL-17 in halothane-induced liver injury

We previously demonstrated that IL-17 is involved in HILI (Kobayashi et al., 2009). To investigate whether E2 or Prog pretreatment affect the production of IL-17, plasma IL-17 level was measured. The IL-17 level was significantly increased only 24 h after the HAL (30 mmol/kg) administration, but not HAL (15 mmol/kg) administration (Fig. 5). E2 or Prog pretreatment alone did not affect the IL-17 levels. As with the expression of inflammatory mediators (Figs. 3 and 4), E2 pretreatment significantly decreased and Prog pretreatment significantly increased the plasma IL-17 levels (Fig. 5). These effects of E2 or Prog were blocked by ICI or RU administration, respectively (Fig. 5).

4. Discussion

Generally, women exhibit worse outcomes from liver injury than men (Lucena et al., 2009; Andrade et al., 2005; Russo et al., 2004). In this study, we focused on two major female sex hormones, E2 and Prog. The circulating levels of E2 and Prog fluctuate as a result of the reproductive phase and pregnancy in women (Wood et al., 2007; Barkley et al., 1979). E2 reduces the severity of various types of liver injuries such as ischemia-reperfusion, trauma-hemorrhage and acetaminophen, but there is little information about the role of Prog in liver injury (Yokoyama et al., 2005; Chandrasekaran et al., 2011; Shimizu et al., 2008). It has been reported that immune-based diseases may have exacerbations during the reproductive phase (Ansar et al., 1985; Ostensen, 1999). Since the activation of immune cells plays an important role in HILI (You et al., 2006; Kobayashi et al., 2009; Cheng et al., 2010), we hypothesized that female sex hormones would affect HILI.

To investigate whether two female sex hormones affect HILI, mice were pretreated with E2 or Prog for 7 days followed by HAL administration. In this study, the E2 and Prog concentrations were

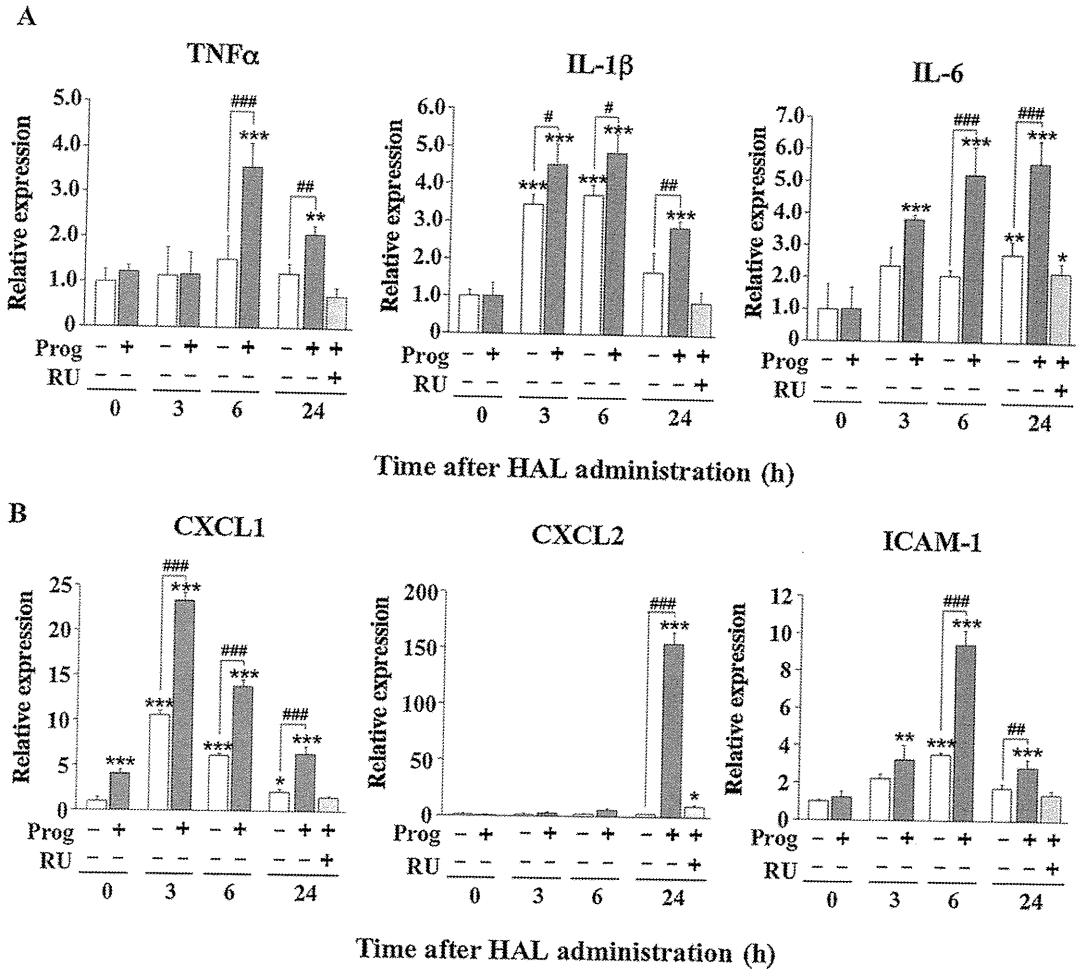

Fig. 4. Time-dependent changes of immune responses by Prog pretreatment in HAL-administered mice. Experimental conditions for animal treatments were the same as those in Fig. 1. Relative expression of hepatic mRNA was measured for proinflammatory cytokines (A) and chemokines and ICAM-1 related to neutrophil infiltration (B) in the Prog-pretreated mouse liver 0, 3, 6 and 24 h after the HAL administration. Expression of hepatic mRNA was normalized to Gapdh mRNA. The data are mean ± SD of 4–5 mice. $^{*}P<0.05$, $^{**}P<0.01$ and $^{***}P<0.001$, campared with CTL. $^{\#}P<0.05$, $^{\#\#}P<0.01$ and $^{\#\#\#}P<0.001$, compared with only HAL-administered mice.

higher in E2 or Prog-pretreated mice than the vehicle treated mice. The plasma E2 levels were 87.72 ± 15.98 pg/mL in mice pretreated with E2 and the plasma Prog levels were 80.43 ± 33.25 ng/mL in mice pretreated with Prog. In general, E2 and Prog secretion increased to maximum during the late pregnancy, plasma E2 level of 60–120 pg/mL and plasma Prog level of 60–120 ng/mL, respectively (Barkley et al., 1979). Therefore, mice pretreated with E2 or Prog in the present study was almost the same as those during

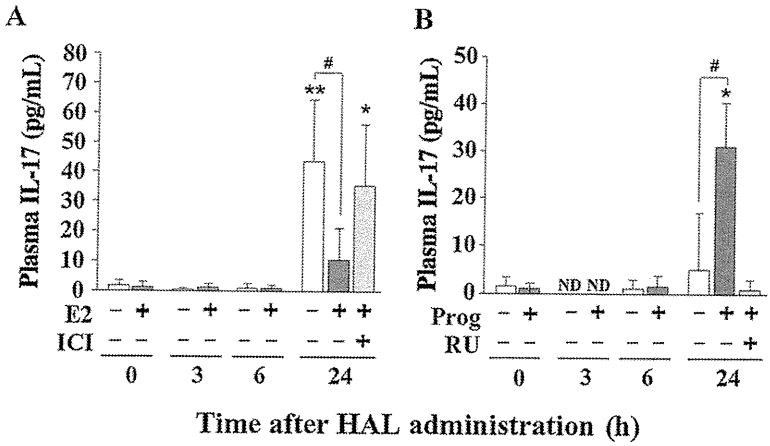

Fig. 5. Time-dependent changes of plasma IL-17 by E2 or Prog pretreatment in HAL-administered mice. Experimental conditions for animal treatments were the same as those in Fig. 1. Plasma IL-17 level was measured in mice pretreated with E2 or Prog 0, 3, 6 and 24 h after the HAL administration (E2; 30 mmol/kg, Prog; 15 mmol/kg). The data are mean ± SD of 4–5 mice. $^{*}P<0.05$ and $^{**}P<0.01$, campared with CTL. $^{\#}P<0.05$, compared with only HAL-administered mice. ND: not detected.

late pregnancy. The transaminase levels and hepatic damage in HILI were attenuated by E2 pretreatment and exacerbated by Prog pretreatment at 24 h but not at 3 and 6 h after the HAL administration (Fig. 1). Neutrophils play a crucial role in the pathology of HILI (You et al., 2006; Kobayashi et al., 2009; Cheng et al., 2010). In this study, MPO-positive cells that infiltrated in the liver were decreased by E2 pretreatment and increased by Prog pretreatment suggesting that E2 and Prog may modulate the degree of HILI via neutrophils. Iso is widely used clinically and shows less hepatotoxicity than HAL (Njoku et al., 1997). No changes in transaminases were observed in mice administered Iso alone. Moreover, Prog pretreatment did not affect the transaminase levels in Iso-administered mice (Fig. 1C). These results indicated that Prog exacerbates the severity of liver injury rather than causing the liver injury. These results may relate to the fact that women exhibit worse outcomes in DILI (Lucena et al., 2009; Andrade et al., 2005; Russo et al., 2004). Moreover, these results indicated that the balance of E2 and Prog changed as a result of the reproductive phase and pregnancy in women affect the severity of DILI.

It has been suggested that TFA–protein adducts caused mild hepatotoxicity and initiated immune reactions (Bourdi et al., 2001; Njoku et al., 1997; Gut et al., 1993). E2 and Prog pretreatment did not affect TFA–protein adduct formation and Cyp2e1 expression (Fig. 2A and B). It was also reported that GSH-depleted guinea pigs exhibited a significant enhancement of HILI (Lind et al., 1992). Recently, it was reported that E2 attenuated APAP-induced liver injury by inhibiting oxidative stress (Chandrasekaran et al., 2011). However, in the present study E2 and Prog pretreatment had no effect on the depletion of the ratio of GSH/GSSG and protein carbonyl contents after HAL administration (Fig. 2C and D). These results indicated that the effects of E2 or Prog may not be involved in the metabolic activation of HAL and oxidative stress. Thus, it is suggested that E2 and Prog are related to another pathway in the pathogenesis of HILI.

Activated immune cells contribute to enhancing liver injury by releasing proinflammatory cytokines and chemokines to further hepatic inflammation, which determines the extent of liver injury (Kaplowitz, 2005; Adams et al., 2010). It has been demonstrated that proinflammatory cytokines, such as TNFα, IL-1β and IL-6, were decreased by E2 pretreatment and enhanced by Prog pretreatment in HILI. In addition, CXC chemokines (CXCL1 and CXCL2) and ICAM-1, which play an important role in neutrophil infiltration, were decreased by E2 pretreatment and enhanced by Prog pretreatment (Figs. 3 and 4). It is reported that transaminase levels achieved peak at 24 h after the HAL administration (You et al., 2006; Kobayashi et al., 2009). Although transaminase levels were not increased at earlier time point (3 or 6 h), the expression levels of TNFα, IL-1β, IL-6, CXCL1 and ICAM-1 were modulated by E2 and Prog pretreatment at earlier time point after HAL administration (Figs. 3 and 4). These results suggested that E2 and Prog affect the severity of HILI by modulating the production of proinflammatory cytokines and chemokines. CXC chemokines and ICAM-1 mRNA expression levels were correlated with neutrophil infiltration and accumulation in the histopathology of HILI (Figs. 1, 3 and 4). CXC chemokines are considered to attract predominantly neutrophils to the liver under stress conditions and the neutrophils undergo adhesion to hepatocytes via hepatocyte ICAM-1 (Ramaiah and Jaeschke, 2007). Furthermore, the roles of neutrophils have been demonstrated in a variety of liver diseases (Ramaiah and Jaeschke, 2007; Li et al., 2004; Frink et al., 2007). It is suggested that these mediators are related to neutrophil infiltration into the liver in HILI.

Interestingly, CXCL1 is increased by Prog pretreatment. CXCL1 not only mediates neutrophil infiltration, but also causes hepatotoxicity effects itself, which lead to massive liver necrosis in preinjured liver (Ramaiah and Jaeschke, 2007; Li et al., 2004; Frink et al., 2007; Stefanovic et al., 2005). In addition, previous studies have demonstrated the important role of CXCL1 in liver injury such as trauma-hemorrhage, endotoxemia and CCl_4-induced liver injury (Shimizu et al., 2008; Ramaiah and Jaeschke, 2007; Li et al., 2004; Frink et al., 2007; Stefanovic et al., 2005). It was also reported that recombinant CXCL1 had no effect in normal liver (Stefanovic et al., 2005). In accordance with these findings, Prog pretreatment had no hepatotoxic effect in normal mice and exacerbated liver injury by HAL administration but not by Iso administration (Fig. 1). We previously reported that IL-17 is involved in HILI (Kobayashi et al., 2009). In this study, changes of IL-17 were correlated with transaminases after HAL administration. E2 or Prog pretreatment alone do not affect the levels of IL-17 (Figs. 1 and 5). Although IL-17 does not initiate an immune response, IL-17 is able to amplify immune response of the early stage (Maione et al., 2009). IL-17-induced immune response was significantly reduced in mice treated with anti-CXCL1 antibody (Maione et al., 2009). Therefore, CXCL1 might play an important role in the progression of HILI by Prog pretreatment in the early stage of immune response.

Previous studies reported that E2 and Prog modulate proinflammatory cytokine production by murine peritoneal macrophages and human mononuclear cells in vitro. These reports also demonstrated that the hormonal effects were mediated by hormonal receptors (Huang et al., 2008; Yuan et al., 2008). In addition, E2 decreased the production of CXCL1 from KC via ER following trauma-hemorrhage (Shimizu et al., 2008). KCs act as the major source of proinflammatory cytokines (TNFα, IL-1β and IL-6) and CXC chemokines under severe stress and various liver injuries (Kaplowitz, 2005; Adams et al., 2010; Laskin, 1990; Mosher et al., 2001). The effects of E2 and Prog on HILI and immune responses were blocked by ICI or RU administration, respectively (Figs. 1, 3 and 4) indicating that the effects of E2 and Prog on HILI could be mediated via ER and PR, respectively. Thus, it might be thought that E2 and Prog affect immune cells responding to E2 and Prog via each receptor, such as monocytes or macrophages, which might result in modulation the immune reaction in HILI.

In conclusions, this study indicated that E2 attenuated and Prog exacerbated the severity of HILI via immune-related reactions. This is the first report that E2 and Prog modulated the severity of HILI. It is also indicated that the E2/Prog hormone balance might represent a risk factor for HILI and that female sex hormones might have a role in one of the mechanism of sex differences in HILI.

Funding

Health and Labor Sciences Research Grants from the Ministry of Health, Labor and Welfare of Japan (H20-BIO-G001).

Conflict of interest

None of the authors has any conflicts of interest related to this manuscript.

Acknowledgement

We thank Mr. Brent Bell for reviewing the manuscript.

References

Adams, D.H., Ju, C., Ramaiah, S.K., Uetrecht, J., Jaeschke, H., 2010. Mechanisms of immune-mediated liver injury. Toxicol. Sci. 115, 307–321.

Andrade, R.J., Lucena, M.I., Fernández, M.C., Pelaez, G., Pachkoria, K., Garciá-Ruiz, E., Garciá-Muñoz, B., González-Grande, R., Pizarro, A., Durán, J.A., Jiménez, M., Rodrigo, L., Romero-Gomez, M., Navarro, J.M., Planas, R., Costa, J., Borras, A., Soler, A., Salmerón, J., Martin-Vivaldi, R., Spanish Group for the Study of Drug-Induced Liver Disease, 2005. Drug-induced liver injury: an analysis of 461 incidences submitted to the Spanish registry over a 10-year period. Gastroenterology 129, 512–521.

Ansar, A.S., Penhale, W.J., Talal, N., 1985. Sex hormones, immune responses, and autoimmune diseases. Mechanisms of sex hormone action. Am. J. Pathol. 121, 531–551.
Barkley, M.S., Geschwind, I.I., Bradford, G.E., 1979. The gestational pattern of estradiol, testosterone and progesterone secretion in selected strains of mice. Biol. Reprod. 20, 733–738.
Björnsson, E., Olsson, R., 2005. Outcome and prognostic markers in severe drug-induced liver disease. Hepatology 42, 481–489.
Bourdi, M., Amouzadeh, H.R., Rushmore, T.H., Martin, J.L., Pohl, L.R., 2001. Halothane-induced liver injury in outbred guinea pigs: role of trifluoracetylated protein adducts in animal susceptibility. Chem. Res. Toxicol. 14, 362–370.
Chalasani, N., Björnsson, E., 2010. Risk factors for idiosyncratic drug-induced liver injury. Gastroenterogy 138, 2246–2259.
Chandrasekaran, V.R., Periasamy, S., Liu, L.L., Liu, M.Y., 2011. 17β-Estradiol protects against acetaminophen-overdose-induced acute oxidative hepatic damage and increases the survival rate in mice. Steroids 76, 118–124.
Cheng, L., You, Q., Yin, J., Holt, M.P., Ju, C., 2010. Involvement of natural killer T cells in halothane-induced liver injury in mice. Biochem. Phamacol. 80, 255–261.
Cousins, M.J., Plummer, J.L., Hall, P.D., 1989. Risk factors for halothane hepatitis. Aust. N. Z. J. Surg. 59, 5–14.
De Valle, M.B., Av Klinteberg, V., Alem, N., Olsson, R., Björnsson, E., 2006. Drug-induced liver injury in a Swedish University hospital out-patient hepatology clinic. Aliment. Pharmacol. Ther. 24, 1187–1195.
Frink, M., Hsieh, Y.C., Hsieh, C.H., Pape, H.C., Choudhry, M.A., Schwacha, M.G., Chaudry, I.H., 2007. Keratiocyte-derived chemokine plays a critical role in the induction of systemic inflammation and tissue damage after trauma-hemorrhage. Shock 28, 576–581.
Griffith, O.W., 1980. Determination of glutathione and glutathione disulfide using glutathione reductase and 2-vinylpyridine. Anal. Biochem. 106, 207–212.
Grossman, C.J., 1985. Interactions between the gonadal steroids and the immune system. Science 227, 257–261.
Gut, J., Christen, U., Huwyler, J., 1993. Mechanisms of halothane toxicity: novel insights. Pharmacol. Ther. 58, 133–155.
Huang, H., He, J., Yin, Y., Aoyagi, E., Takenaka, H., Itagaki, T., Sannomiya, K., Tamaki, K., Harada, N., Shono, M., Shimizu, I., Takayama, T., 2008. Opposing effects of estradiol and progesterone on the oxidative stress-induced production of chemokine and proinflammatory cytokines in murine peritoneal macrophages. J. Med. Invest. 55, 133–141.
Inman, W.H., Mushin, W.W., 1974. Jaundice after repeated exposure to halothane: analysis of reports to the committee on safety of medicines. Br. Med. J. 1, 5–10.
Kaplowitz, N., 2005. Idiosyncratic drug hepatotoxicity. Nat. Rev. Drug Discov. 4, 489–499.
Kobayashi, E., Kobayashi, M., Tsuneyama, K., Fukami, T., Nakajima, M., Yokoi, T., 2009. Halothane-induced liver injury is mediated by interleukin-17 in mice. Toxicol. Sci. 111, 302–310.
Kumada, T., Tsuneyama, K., Hatta, H., Ishizawa, S., Takano, Y., 2004. Improved 1-h rapid immunostaining method using intermittent microwave irradiation: practicability based on 5 years application in Toyama Medical and pharmaceutical University Hospital. Mod. Pathol. 17, 1141–1149.
Laskin, D.L., 1990. Nonparenchymal cells and hepatotoxicity. Semin. Liver Dis. 10, 293–304.
Li, A.P., 2002. A review of the common properties of drugs with idiosyncratic hepatotoxicity and the "multiple determinant hypothesis" for the manifestation of idiosyncratic drug toxicity. Chem. Biol. Interact. 142, 7–23.
Li, X., Klintman, D., Liu, Q., Sato, T., Jeppsson, B., Thorlacius, H., 2004. Critical role of CXC chemokines in endotoxemic liver injury in mice. J. Leukoc. Biol. 75, 443–452.
Lind, R.C., Gandolfi, A.J., Hall, P.M., 1992. Glutathione depletion enhances subanesthetic halothane hepatotoxicity in guinea pigs. Anesthesiology 77, 721–727.
Lucena, M.I., Andrade, R.J., Kaplowitz, N., García-Cortes, M., Fernández, M.C., Romero-Gomez, M., Bruguera, M., Hallal, H., Robels-Diaz, M., Rodriguez-González, J.F., Navarro, J.M., Salmeron, J., Martinez-Odriozola, P., Pérez-Alvarez, R., Borraz, Y., Hidalgo, R., Spanish Group for the Study of Drug-induced Liver Disease, 2009. Phenotypic characterization of idiosyncratic drug-induced liver injury: the influence of age and sex. Hepatology 49, 2001–2009.
Maione, F., Paschalidis, N., Mascolo, N., Dufton, N., Perretti, M., D'Acquisto, F., 2009. Interleukin 17 sustains rather than induces inflammation. Biochem. Pharmacol. 77, 878–887.
Mosher, B., Dean, R., Harkema, J., Remick, D., Palma, J., Crockett, E., 2001. Inhibition of kupffer cells reduced CXC chemokine production and liver injury. J. Surg. Res. 99, 201–210.
Njoku, D., Laster, M.J., Gong, D.H., Eger, E.I.2nd., Reed, G.F., Martin, J.L., 1997. Biotransformation of halothane, enflurane, isoflurane, and desflurane to trifluoroacetylated liver proteins: association between protein acylation and hepatic injury. Anesth. Analg. 84, 173–178.
Ostapowicz, G., Fontana, R.J., Schiødt, F.V., Larson, A., Davern, T.J., Han, S.H., McCashland, T.M., Shakil, A.O., Hay, J.E., Hynan, L., Crippin, J.S., Blei, A.T., Samuel, G., Reisch, J., Lee, W.M., U.S. Acute Liver Filure Study Group, 2002. Results of a prospective study of acute liver failure at 17 tertiary care centers in the United States. Ann. Intern. Med. 137, 947–954.
Ostensen, M., 1999. Sex hormones and pregnancy in rheumatoid arthritis and systemic lupus erythematosus. Ann. N. Y. Acad. Sci. 876, 131–143.
Ramaiah, S.K., Jaeschke, H., 2007. Role of neutrophils in the pathogenesis of acute inflammatory liver injury. Toxicol. Pathol. 35, 757–766.
Ray, D.C., Drummond, G.B., 1991. Halothane hepatitis. Br. J. Anaethsiol. 67, 84–99.
Russo, M.W., Galanko, J.A., Shrestha, R., Fried, M.W., Watkins, P., 2004. Liver transplantation for acute liver failure from drug induced liver injury in the United States. Liver Transpl. 10, 1018–1023.
Shimizu, T., Suzuki, T., Yu, H., Yokoyama, Y., Choudhry, M.A., Bland, K.I., Chaudry, I.H., 2008. The role of estrogen receptor subtypes on hepatic neutrophil accumulation following trauma-hemorrhage: direct modulation of CINC-1 production by kupffer cells. Cytokine 43, 88–92.
Stefanovic, L., Brenner, D.A., Stefanovic, B., 2005. Direct hepatotoxic effect of KC chemokaine in the liver without infiltration of neutrophils. Exp. Biol. Med. 230, 573–586.
Sugaya, A., Sugiyama, T., Yanase, S., Shen, X.X., Minoura, H., Toyoda, N., 2000. Expression of glucose transporter 4 mRNA in adipose tissue and skeletal muscle of ovariectomized rats treated with sex steroid hormones. Life Sci. 66, 641–648.
Tietze, F., 1969. Enzymatic method for quantitative determination of nanogram amounts of total and oxidized glutathione: applications to mammalian blood and other tissues. Anal. Biochem. 27, 502–522.
Wood, G.A., Fata, J.E., Watson, K.L., Khokha, R., 2007. Circulating hormones and estrous stage predict cellular and stromal remodeling in murine uterus. Reproduction 133, 1035–1044.
You, Q., Cheng, L., Reilly, T.P., Wegmann, D., Ju, C., 2006. Role of neutrophils in a mouse model of halothane-induced liver injury. Hepatology 44, 1421–1431.
Yuan, Y., Shimizu, I., Shen, M., Aoyagi, E., Takenaka, H., Itagaki, T., Urada, M., Sannomiya, K., Kohno, N., Shuno, M., Takayama, T., 2008. Effects of estradiol and progesterone on the proinflammatory cytokine production by mononuclear cells from patients with chronic hepatitis C. World J. Gastroenterol. 14, 2200–2207.
Yokoyama, Y., Nimura, Y., Nagio, M., Bland, K.I., Chaudry, I.H., 2005. Current understanding of gender dimorphism in hepatic pathophysiology. J. Surg. Res. 128, 147–156.

0090-9556/11/3907-1303–1310$25.00
DRUG METABOLISM AND DISPOSITION

DMD 39:1303–1310, 2011

Vol. 39, No. 7
38661/3699032
Printed in U.S.A.

In Vitro Investigation of the Glutathione Transferase M1 and T1 Null Genotypes as Risk Factors for Troglitazone-Induced Liver Injury[S]

Toru Usui, Takanori Hashizume, Takashi Katsumata, Tsuyoshi Yokoi, and Setsuko Komuro

Pharmacokinetics Research Laboratories, Dainippon Sumitomo Pharma Co., Ltd., Osaka, Japan (T.U., T.H., T.K., S.K.); and Drug Metabolism and Toxicology, Faculty of Pharmaceutical Sciences, Kanazawa University, Kanazawa, Japan (T.U., T.Y.)

Received February 8, 2011; accepted April 21, 2011

ABSTRACT:

The double null mutation of glutathione transferase, GSTM1 and GSTT1, is reported to influence troglitazone-associated abnormal increases of alanine aminotransferase and aspartate aminotransferase. However, no nonclinical data with a bearing on the clinical outcomes and underlying mechanisms have hitherto been reported. To investigate whether deficiency in GSTM1 and/or GSTT1 is related to troglitazone hepatotoxicity in vitro, the covalent binding level (CBL) (an index of reactive metabolite formation) and cytotoxicity of troglitazone and rosiglitazone, another thiazolidinedione but with low hepatotoxicity, were examined using human liver samples phenotyped for cytochrome P450s and genotyped for GSTM1 and GSTT1. Despite addition of GSH, CBLs of troglitazone and rosiglitazone in human liver microsomes were correlated with CYP3A (or CYP2C8) and CYP2C8 activities, respectively. With addition of recombinant GSTM1, the microsomal CBLs of troglitazone and rosiglitazone decreased. However, the CBLs of troglitazone in GSTM1/GSTT1 wild-type hepatocytes were unexpectedly higher than those in null hepatocytes. Although this discrepancy has not been fully explained, the GSTM1 and GSTT1 null mutations increased the cytotoxicity of troglitazone, independent of CYP3A or CYP2C8 activities. Furthermore, a GSH adduct of troglitazone, M2, limited to GSTM1 wild-type hepatocytes was detected. Of clear interest, GSTM1 and/or GSTT1 null mutation-dependent cytotoxicity and higher exposure to the reactive metabolite trapped as M2 as for troglitazone were not observed for rosiglitazone. This result might at least partly explain the findings related to clinical hepatotoxicity, suggesting that measurement of GSH adducts or cytotoxicity using GSTM1- and GSTT1-genotyped hepatocytes might offer an important in vitro system to assist in better prediction of idiosyncratic hepatotoxicity.

Introduction

Troglitazone (Rezulin) (Fig. 1) was the first thiazolidinedione peroxisome proliferator-activated receptor γ agonist developed for the treatment of type II diabetes (Fujiwara et al., 1995; Sparano and Seaton, 1998). It was also the first in its class approved by the U.S. Food and Drug Administration for marketing in 1997 but was subsequently found to induce severe idiosyncratic hepatotoxicity in rare instances (Gitlin et al., 1998; Shibuya et al., 1998), which led to its withdrawal from the market in 2000. In the meantime, reports of usually milder and reversible hepatotoxicity have been documented very rarely with other thiazolidinediones, such as rosiglitazone (Avandia) (Fig. 1) and pioglitazone (Actos) (Isley, 2003). As a particularly interesting example for research on drug-induced liver injury (DILI), numerous researchers have investigated the mechanisms of troglitazone hepatotoxicity.

Although troglitazone hepatotoxicity was not predicted from tests in conventional experimental animals (Watanabe et al., 1999), some cellular events induced by troglitazone may have contributed to the clinically observed hepatotoxicity, for example, 1) reactive metabolite formation by oxidative cytochrome P450 (P450) 3A-mediated metabolism (Kassahun et al., 2001; Tettey et al., 2001; Yamamoto et al., 2002; He et al., 2004), 2) inhibition of the hepatic drug transporter, bile salt export pump or organic anion-transporting polypeptide by troglitazone sulfate (Funk et al., 2001a; Nozawa et al., 2004), 3) mitochondria-mediated toxicity by unchanged troglitazone (Masubuchi et al., 2006; Lim et al., 2008), 4) troglitazone-mediated apoptosis (Bae and Song, 2003; Shiau et al., 2005), and 5) down-regulation of proinflammatory cytokines in Kupffer cells (Sigrist et al., 2000). Although these nonclinical data cannot explain the idiosyncratic nature of troglitazone hepatotoxicity, high activity of drug-metabolizing enzymes (e.g., P450s) that form reactive metabolites or low activity of detoxification enzymes (e.g., glutathione transferases) (GSTs), which are responsible for scavenging reactive metabolites, are likely to be risk factors. In fact, with regard to this idiosyncrasy, there was a solitary and notable report indicating that the double mutation of GSTM1 and GSTT1 was associated with abnormally high levels of

Article, publication date, and citation information can be found at http://dmd.aspetjournals.org.
doi:10.1124/dmd.111.038661.
[S] The online version of this article (available at http://dmd.aspetjournals.org) contains supplemental material.

ABBREVIATIONS: DILI, drug-induced liver injury; P450, cytochrome P450; GST, glutathione transferase; ALT, alanine aminotransferase; AST, aspartate aminotransferase; CBL, covalent binding level; rh, recombinant human; HPLC, high-performance liquid chromatography; LC, liquid chromatography; MS/MS, tandem mass spectrometry; MRM, multiple reaction monitoring; UGT, UDP-glucuronosyltransferase; SULT, sulfotransferase; HLA, human leukocyte antigen.

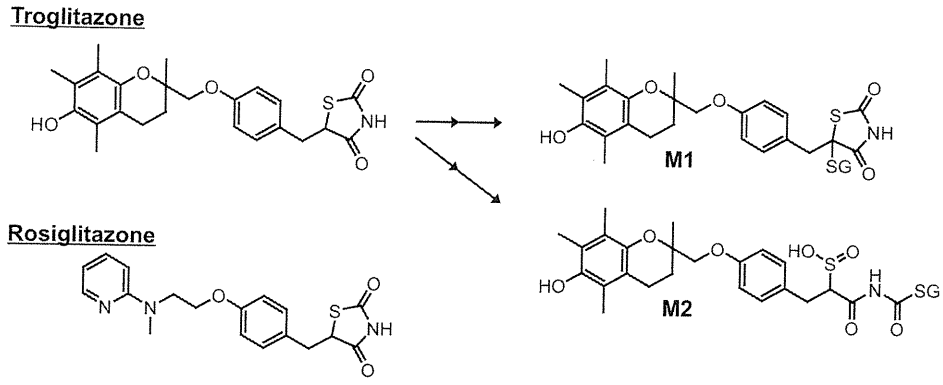

FIG. 1. Structures of troglitazone, rosiglitazone, and two postulated troglitazone GSH adducts. –SG, glutathione.

ALT and AST after administration of troglitazone on retrospective analysis using clinical samples (Watanabe et al., 2003). However, to our knowledge, no nonclinical data to link with the clinical outcomes and provide more detailed clues to mechanisms have hitherto been reported.

The purpose of the present study was to investigate whether GSTM1 and/or GSTT1 defects are involved in troglitazone hepatotoxicity in vitro. It is clear that metabolic activation of a drug to reactive metabolites and subsequent covalent binding to target macromolecules might be a necessary first step in the generation of idiosyncratic drug reactions in many cases (Walgren et al., 2005). We have already reported that covalent binding is one risk factor for DILI (Usui et al., 2009). Therefore, the covalent binding levels (CBLs) (an index of reactive metabolite formation) of troglitazone and rosiglitazone (as a negative control) were investigated using human in vitro liver samples with a diversity of P450 phenotypes or GST genotypes. Furthermore, cytotoxicity was also investigated to cast light on the idiosyncrasy of troglitazone hepatotoxicity.

Materials and Methods

Materials. [^{14}C]Troglitazone and [^{14}C]rosiglitazone were synthesized in-house. Unlabeled troglitazone and rosiglitazone were purchased from Toronto Research Chemicals Inc. (North York, ON, Canada). Pooled human liver microsomes (mixed-gender pool of 50 individuals) and 16 individual human liver microsome samples (Reaction Phenotyping Kit, version 7) were obtained from XenoTech, LLC (Lenexa, KS). Cryopreserved human hepatocytes were purchased from In Vitro Technologies, Inc. (Baltimore, MD) or XenoTech, LLC. The activities of major drug-metabolizing enzymes in microsomes and hepatocytes had been measured by the suppliers. Use of human samples in this study was approved by the ethics committee of the Drug Research Division, Dainippon Sumitomo Pharma Co., Ltd. (Osaka, Japan). Recombinant human (rh) GSTA1 and rhGSTM1, used in Fig. 2 (cytosol isolated from *Escherichia coli*-expressing human GSTA1 and GSTM1, respectively), and control cytosol (isolated from *E. coli* host strain) were purchased from Cypex Ltd. (Dundee, UK). rhGSTA1, rhGSTM1, and rhGSTP1, used in Supplemental Fig. 2, were purchased from PanVera Corp. (Madison, WI). To prepare the negative control of PanVera rhGST, rhGSTM1 was heat-inactivated at 90°C for 2 min. NADPH and reduced GSH were from Oriental Yeast Co., Ltd. (Tokyo, Japan), and Nacalai Tesque, Inc. (Kyoto, Japan), respectively. All other regents and solvents were of the highest grade commercially available.

Incubation Using Human Liver Microsomes. In microsomal assays, radiolabeled troglitazone and rosiglitazone (final concentration 10 μM) were incubated with 1 mg/ml pooled human liver microsomes or 16 individual human liver microsome samples phenotyped for P450 activities in the presence of 1 mM NADPH and 1 mM GSH at 37°C for 1 h in 500 μl of a reaction mixture consisting of 50 mM phosphate buffer (pH 7.4). rhGSTA1, rhGSTM1, rhGSTP1, or control cytosol (0.4 mg/ml) was added as required.

Genotyping for GSTM1 and GSTT1 Using Human Hepatocytes. GSTM1 and GSTT1 genotyping was performed by polymerase chain reaction amplification of genomic DNA as described previously (Arand et al., 1996). Genomic DNA was isolated from human hepatocytes using a DNeasy Blood and Tissue Kit (QIAGEN, Hilden, Germany).

Incubation Using Cryopreserved Human Hepatocytes for Measurement of CBL and Metabolite Analysis. Radiolabeled compounds (10 μM) were incubated with cryopreserved human hepatocytes (1 × 10^6 cells/ml) genotyped for GSTM1 and GSTT1 at 37°C for 8 h under an atmosphere of

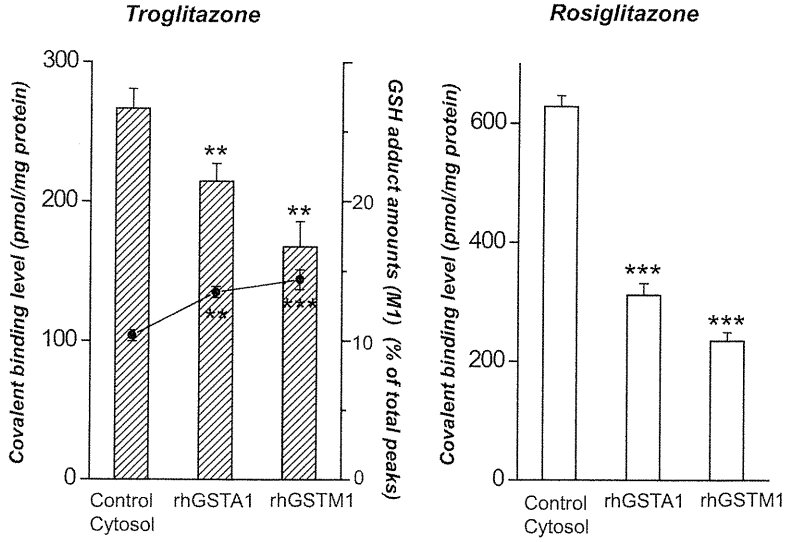

FIG. 2. Effect of rhGSTA1 or rhGSTM1 on CBLs and a GSH adduct in human liver microsomes. Radiolabeled troglitazone and rosiglitazone (10 μM) were incubated with pooled human liver microsomes and with control cytosol (isolated from *E. coli* host strain, left bars), rhGSTA1 (recombinant human GSTA1 expressed in *E. coli*, middle bars), or rhGSTM1 (right bars) in the presence of 1 mM NADPH and 1 mM GSH at 37°C for 1 h followed by determination of CBLs. The eluates were analyzed by radio-HPLC, and the amounts of M1 (the main GSH adduct of troglitazone in this assay) are shown (●). No appreciable GSH adducts of rosiglitazone were found with radio-HPLC. The CBL and GSH adduct data are the means ± S.D. from three assays. **, $p < 0.01$; ***, $p < 0.001$, significantly different from control cytosol.

95% air- 5% CO_2 in 300-μl suspensions of hepatocytes in incubation medium (XenoTech, LLC).

Measurement of CBL. CBL was measured according to the method we reported previously (Usui et al., 2009). Reactions of microsomes and hepatocytes were stopped by addition of ice-cold methanol. For measurement of radioactivity bound to proteins, the reaction mixtures after precipitation were loaded onto glass fiber filters and washed with 80% (v/v) methanol and acetonitrile to remove unbound radioactivity. The first filtrate was used for radio-high-performance liquid chromatography (HPLC) analysis or liquid chromatography (LC)-tandem mass spectrometry (MS/MS) analysis of metabolites unbound to proteins as described below. The filter was transferred to a scintillation vial with 10% SDS and incubated overnight at 55°C to dissolve proteins. The radioactivity and protein concentration were then measured. The CBL was calculated from the following equation:

$$\frac{\text{Radioactivity in the protein solution (dpm/ml)}}{\text{Specific radioactivity of substrate (dpm/pmol)}} \times \text{Protein concentration in the protein solution (mg/ml)}$$

Radio-HPLC and LC-MS/MS Analyses. The first filtrate from the glass fiber filters was collected and evaporated to dryness, and the residue was dissolved in the mobile phase and loaded onto an Inertsil ODS-3 column (3-μm, 2.1 i.d. × 150 mm; GL Science, Inc., Tokyo, Japan) with a column temperature of 40°C. The LC system consisted of an Agilent 1200 (Agilent Technologies, Santa Clara, CA) pump set at a flow rate of 0.25 ml/min. The mobile phase to detect GSH adducts of troglitazone consisted of a linear gradient of solvent A (0.1% formic acid) and solvent B (acetonitrile) according to the following program: 20% B (0 min) to 30% B (5 min) to 35% B (26 min) to 100% B (30 min). The mobile phase to investigate metabolite profiling of troglitazone consisted of a linear gradient of solvent A (0.1% formic acid) and solvent B (acetonitrile) according to the following program: 20% B (0 min) to 30% B (5 min) to 35% B (35 min) to 40% B (55 min) to 100% B (65 min). The mobile phase to investigate metabolite profiling of rosiglitazone consisted of a linear gradient of solvent A (10 mM ammonium acetate) and solvent B (acetonitrile) according to the following program: 5% B (0 min) to 35% B (20 min) to 60% B (35 min) to 100% B (40 min). Radioactivity was detected with a flow scintillation detector (Radiomatic 610TR; PerkinElmer Life and Analytical Sciences, Waltham, MA), using Ultima Flo-M scintillation cocktail (PerkinElmer Life and Analytical Sciences). Mass analysis was conducted on a 4000 QTRAP hybrid triple quadrupole-linear ion trap mass spectrometer (Applied Biosystems, Foster City, CA) equipped with an electrospray ion source for detection of GSH adducts of troglitazone, M1 and M2 (Fig. 1). Ionization parameters included an ion spray voltage of −4100 V and source temperature of 200°C. M1 and M2 were identified by means of multiple reaction monitoring (MRM) in the negative ion mode [MRM transitions: M1, $[M - H]^-$ (deprotonated molecule) = 745 → 272; M2, $[M - H]^-$ = 779 → 272]. MRM parameters of M1 and M2 included a declustering potential of −60 V and collision energy of −35 V. Molecular masses of other metabolites of troglitazone and rosiglitazone were determined as described in our previous article (Usui et al., 2009).

Measurement of ATP Levels in Hepatocytes. Troglitazone and rosiglitazone were incubated with cryopreserved human hepatocytes (1×10^5 cells/ml) genotyped for GSTM1 and GSTT1 at 37°C for 2 h under an atmosphere of 95% air-5% CO_2 in 100-μl suspensions of hepatocytes in incubation medium (XenoTech, LLC). ATP levels were measured using a CellTiter-Glo Luminescent cell viability kit from Promega (Madison, WI). This assay generates luminescent signals by luciferase reactions that are proportional to the amount of ATP present.

Statistical Analysis. All statistical analyses were performed using SAS Enterprise Guide 4.1 (SAS Institute, Cary, NC). Correlations between CBLs or unchanged drug amounts and specific P450 activities in human liver microsomes or hepatocytes were analyzed using linear regression analysis. The two-way analyses of variance were used to test the effect of the GSTM1 genotype and GSTT1 genotype on CBLs or on remaining unchanged drug amounts. Student's t test was used to compare the cytotoxicity of troglitazone and rosiglitazone between GSTM1/GSTT1 null and wild-type hepatocytes and to compare the CBL or M1 amounts with addition between rhGSTs and control cytosol.

Results

Correlation between CBLs and P450 Activities of Human Liver Microsomes from Individuals. CBLs of troglitazone and rosiglitazone with 16 individual human liver microsomes phenotyped for enzymatic activities of P450s were investigated in the presence of 1 mM GSH. The average absolute values were 297 and 435 pmol/mg protein, respectively. Despite addition of GSH as a scavenger, individual microsomes showed large variation in CBLs. Compared with the individual CBLs of troglitazone (152–529 pmol/mg), those of rosiglitazone (141–1013 pmol/mg) varied more widely. The coefficient of variation of CBL was 38% for troglitazone and 46% for rosiglitazone. Correlations between CBLs and P450 activities are shown in Table 1. CBLs of troglitazone were significantly and positively correlated with CYP3A activities ($r = 0.89$, $p < 0.001$, testosterone 6β-hydroxylation; $r = 0.83$, $p < 0.001$, midazolam 1′-hydroxylation). Furthermore, CBLs of troglitazone were also positively correlated with CYP2C8 activities ($r = 0.60$, $p = 0.01$). Meanwhile, CBLs of rosiglitazone were significantly and positively correlated with CYP2C8 activities ($r = 0.65$, $p = 0.005$).

TABLE 1

Correlation between CBLs and P450 activities of human liver microsomes from 16 individuals

Radiolabeled troglitazone and rosiglitazone (10 μM) were incubated with 16 individual human liver microsomes in the presence of 1 mM NADPH and 1 mM GSH at 37°C for 1 h followed by determination of CBLs. Experiments were conducted in duplicate and correlation (R) between the means of CBLs and P450 activities was analyzed.

P450 Activities	R value (p)	
	CBLs of Troglitazone	CBLs of Rosiglitazone
CYP1A2 (7-ethoxyresorufin O-dealkylation)	0.08 (0.76)	0.09 (0.73)
CYP1A2 (phenacetin O-deethylation)	0.27 (0.30)	0.10 (0.69)
CYP2A6 (coumarin 7-hydroxylation)	0.22 (0.40)	0.0002 (0.99)
CYP2B6 (*S*-mephenytoin N-demethylation)	0.51 (0.05)	0.18 (0.50)
CYP2B6 (bupropion hydroxylation)	0.31 (0.23)	0.08 (0.76)
CYP2C8 (paclitaxel 6α-hydroxylation)	0.60 (0.01)*	0.65 (0.005)**
CYP2C9 (diclofenac 4′-hydroxylation)	0.05 (0.86)	0.11 (0.67)
CYP2C19 (*S*-mephenytoin 4′-hydroxylation)	0.16 (0.55)	−0.05 (0.85)
CYP2D6 (dextromethorphan O-demethylation)	0.37 (0.14)	0.06 (0.82)
CYP2E1 (chlorzoxazone 6-hydroxylation)	−0.02 (0.94)	0.04 (0.87)
CYP3A4/5 (testosterone 6β-hydroxylation)	0.89 (<0.001)***	0.24 (0.36)
CYP3A4/5 (midazolam 1′-hydroxylation)	0.83 (<0.001)***	0.21 (0.43)
CYP4A11 (lauric acid 12-hydroxylation)	0.07 (0.80)	0.39 (0.13)

* Significant at $p < 0.05$.
** Significant at $p < 0.01$.
*** Significant at $p < 0.001$.

DRUG METABOLISM AND DISPOSITION DMD aspet

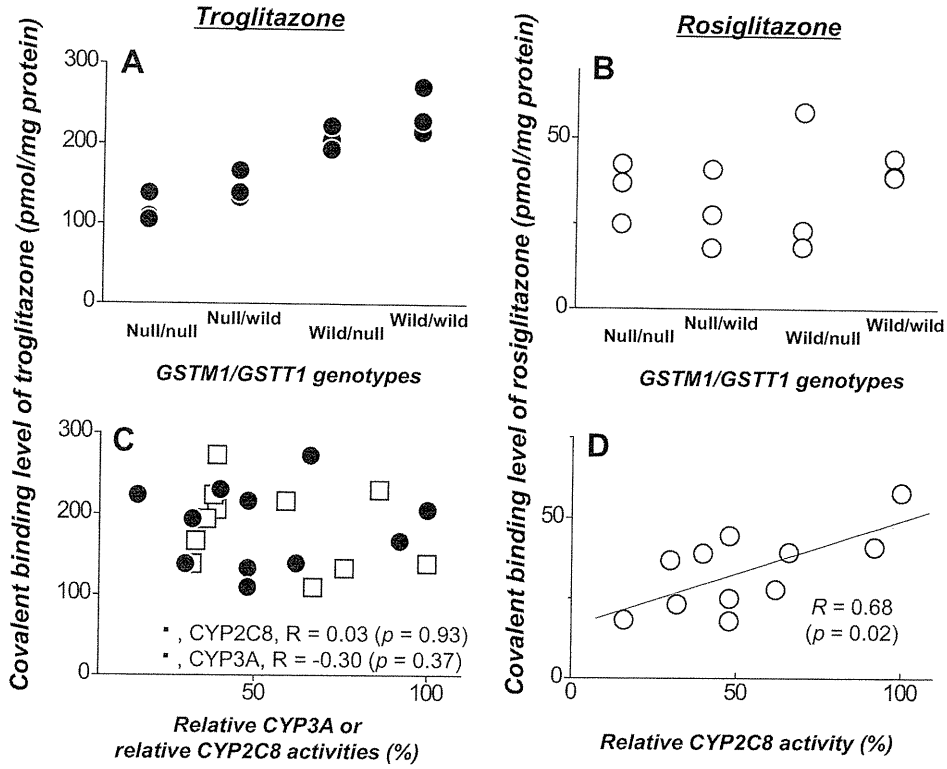

FIG. 3. Comparison of CBLs in GSTM1/GSTT1 null and wild-type hepatocytes. Radiolabeled troglitazone (A and C) and rosiglitazone (B and D) (10 μM) were incubated with 12 cryopreserved human hepatocytes genotyped for GSTM1 and GSTT1 null mutations and phenotyped for P450 activity at 37°C for 8 h followed by determination of CBLs. Two-way analysis of variance results for GSTM1 genotype and for GSTT1 genotype affecting CBLs were shown in Table 3.

Effects of rhGSTA1 or rhGSTM1 on CBLs in Human Liver Microsomes. The scavenging effects of rhGSTA1 or rhGSTM1 (from Cypex Ltd.) on CBLs of troglitazone and rosiglitazone mediated by pooled human liver microsomes were investigated in the presence of 1 mM GSH (Fig. 2). With addition of rhGSTA1 or rhGSTM1, microsomal CBLs of troglitazone and rosiglitazone were significantly decreased compared with those after addition of control cytosol. Furthermore, the GSH adduct of a troglitazone-reactive metabolite reported as 5-glutathionyl-thiazolidine-2,4-dione (M1, Fig. 1) in a previous publication (He et al., 2004) was increased by addition of rhGSTA1 or rhGSTM1 in radio-HPLC analysis (A representative radiochromatogram of troglitazone is shown in Supplemental Fig. 1A.) rhGSTA1 and rhGSTM1 did not affect the decrease in unchanged troglitazone in radio-HPLC analysis (data not shown). Meanwhile, no appreciable GSH adducts of rosiglitazone were found in radio-HPLC.

Correlation between CBLs and GSTM1/GSTT1 Genotypes in Individual Human Hepatocytes. Fifty-nine individual human hepatocytes were genotyped for GSTM1 and GSTT1 null mutations. Three each were selected for each of the four genotypes of GSTM1/GSTT1 (wild/wild, wild/null, null/wild, and null/null) (total 12 lots). With use of the genotyped 12 individual human hepatocytes, CBLs of troglitazone and rosiglitazone were investigated (Fig. 3). Characterizations of individual hepatocytes regarding drug-metabolizing enzymes are shown in Table 2. CBLs of troglitazone were higher than those of rosiglitazone in most of the hepatocytes used (Fig. 3, A and B). CBLs of troglitazone varied widely and independently of the activities of CYP3A and CYP2C8 (Fig. 3C), which are involved in reactive metabolite formation of troglitazone in microsomes (Table 1). CBLs of rosiglitazone in hepatocytes correlated with CYP2C8 activities ($r = 0.68$, $p = 0.02$) (Fig. 3D). In contrast to the result of a microsomal assay using rhGSTM1, CBLs of troglitazone in GSTM1 or GSTT1 null hepatocytes tended to be lower than those in GSTM1 or GSTT1 wild-type hepatocytes (Fig. 3A). As the result of two-way analyses of variance to consider the interaction term (Table 3), both the GSTM1 genotype and GSTT1 genotype significantly affected CBLs of troglitazone ($F = 54.73$, $p < 0.001$ and $F = 6.44$, $p = 0.03$, respectively) without the interaction term. On the other hand, neither GSTM1genotype nor GSTT1 genotype significantly affected CBLs of rosiglitazone ($F = 0.47$, $p = 0.51$ and $F = 0.02$, $p = 0.90$, respectively) without the interaction term.

Correlation between Remaining Unchanged Drugs and GSTM1/GSTT1 Genotypes in Individual Human Hepatocytes. Remaining unchanged drug amounts of troglitazone and rosiglitazone were investigated by radio-HPLC analysis from filtrates after an 8-h incubation with 12 individual human hepatocytes. Representative radiochromatograms of troglitazone and rosiglitazone are shown in Supple-

TABLE 2

Characterization of individual hepatocytes for drug-metabolizing enzymes in the CBL determination assay (lots A–L) and the cytotoxicity assay (lots A, B, J, and K)

Activities of CYP3A (formation rate of 6β-hydroxylated testosterone), CYP2C8 (4′-methylhydroxyl tolbutamide), SULT (7-hydroxycoumarine sulfate), and UGT (7-hydroxycoumarine glucuronide) were measured by the suppliers.

Lot	GSTM1/GSTT1 Genotypes	Enzymatic Activity			
		CYP3A	CYP2C8	SULT	UGT
		pmol/10^6 cell/min			
A	Wild/wild	152	24	31	129
B	Wild/wild	100	33	9	109
C	Wild/wild	223	20	16	432
D	Wild/null	102	50	9	108
E	Wild/null	94	16	110	415
F	Wild/null	99	8	29	444
G	Null/wild	197	24	33	540
H	Null/wild	259	31	34	508
I	Null/wild	85	46	8	86
J	Null/null	174	24	42	366
K	Null/null	82	15	14	118
L	Null/null	188	No data	No data	No data

DMD DRUG METABOLISM AND DISPOSITION aspet

TABLE 3

Two-way analysis of variance results for GSTM1 genotype and for GSTT1 genotype affecting CBLs of troglitazone and rosiglitazone

Source	Troglitazone			Rosiglitazone		
	Mean Square	*F*	*p*	Mean Square	*F*	*p*
GSTM1	25034.5	57.43***	<0.001	80.6	0.47	0.51
GSTT1	2806.0	6.44*	0.03	2.9	0.02	0.90
Interaction	7.2	0.02	0.90	139.4	0.81	0.39

* Significant at $p < 0.05$.
*** Significant at $p < 0.001$.

mental Fig. 1, B and C. Remaining unchanged troglitazone amounts in GSTM1 null hepatocytes tended to be higher than those in GSTM1 wild-type hepatocytes (Fig. 4A). As shown by two-way analyses of variance (Table 4), the GSTM1 genotype significantly affected remaining unchanged troglitazone amounts ($F = 8.25$, $p = 0.02$) without the interaction term. The remaining unchanged troglitazone amounts between GSTT1 null and wild-type hepatocytes were not significantly different ($F = 2.85$, $p = 0.13$). On the other hand, neither the GSTM1genotype nor the GSTT1 genotype significantly affected remaining unchanged rosiglitazone amounts ($F = 0.00$, $p = 0.99$ and $F = 2.54$, $p = 0.15$, respectively) without the interaction term (Fig. 4B; Table 4). The stability of [^{14}C]troglitazone and [^{14}C]rosiglitazone under these assay conditions was investigated by radio-HPLC. Troglitazone and rosiglitazone were stable at 10 or 50 μM in hepatocyte incubation medium for 8 h. Saha et al. (2010) reported that troglitazone sulfate was stable under conditions similar to those in our study, and thus troglitazone sulfate was not considered to be deconjugated to unchanged troglitazone.

Troglitazone GSH Adducts (M1 and M2) in GSTM1- and GSTT1-Genotyped Hepatocytes and Substrate Selectivity for the GSH Adducts with the GST Isoforms. GSH adducts of troglitazone were detected by LC-MS/MS analysis from filtrates after incubation with 12 individual human hepatocytes genotyped for GSTM1 and GSTT1 (Fig. 5). The most notable, M1, was identified with all genotypes. However, M2, which is a GSH conjugate of isocyanate or isothiocyanate, the latter involving a novel oxidative scission of the thiazolidinedione ring system (Fig. 1) (Kassahun et al., 2001), was scarcely obtained with GSTM1 null hepatocytes. No appreciable GSH adducts of rosiglitazone were found with any of the genotypes in this study. The substrate selectivity for troglitazone-reactive metabolites trapped as M1 or M2 was verified by incubation of troglitazone with human liver microsomes using rhGSTA1, rhGSTM1, and rhGSTP1 from PanVera Corp. in the presence of 1 mM GSH. LC-MS/MS analysis for detection of GSH adducts, M1 and M2, by means of the MRM method showed that all isoforms (rhGSTA1, rhGSTM1, and rhGSTP1) increased the formation of M1. On the other hand, only rhGSTM1 increased the formation of M2 (Supplemental Fig. 2).

Cytotoxicity Assays in Individual Human Hepatocytes. Data for ATP levels in individual cryopreserved human hepatocytes, genotyped for GSTM1 and GSTT1, after treatment with troglitazone and rosiglitazone are summarized in Fig. 6. CYP3A and CYP2C8 activities, which affect reactive metabolite formation of troglitazone and rosiglitazone (Table 1), were comparable among the hepatocytes in this assay (Table 2). Treatment of GSTM1 and GSTT1 null hepatocytes with 50 μM troglitazone markedly reduced ATP levels compared with those for the no drug control. In contrast, no such reduction was evident in GSTM1 and GSTT1 wild-type hepatocytes exposed to troglitazone. ATP depletion was independent of UDP-glucuronosyltransferase (UGT) and sulfotransferase (SULT) activities (Table 2). Rosiglitazone did not change the cellular ATP concentration with any of the genotypes.

Discussion

"Metabolic idiosyncrasy" and/or "immune idiosyncrasy" are believed to cause DILI (Uetrecht, 2009). Troglitazone-induced liver injury that is not associated with any fever, rash, eosinophilia, or antidrug antibodies (nonallergic hepatotoxicity) has been considered to belong to the category of metabolic idiosyncrasy. Interindividual differences in drug-metabolizing enzymes derived from polymorphisms that lead to greater exposure to reactive metabolites may be one possible explanation for the idiosyncratic nature of this nonallergic hepatotoxicity (Russmann et al., 2010). Conventional animal experiments would not be expected to be able to reproduce troglitazone hepatotoxicity because of the lack of the genetic variation. In this study, we focused on the metabolic idiosyncrasy of troglitazone hepatotoxicity and tried to investigate the mechanism with human in vitro samples featuring high genetic diversity.

In 16 individual microsomal experiments, CBLs of troglitazone were significantly correlated with CYP3A or CYP2C8 activities despite addition of GSH, which is a scavenger of reactive metabolites (Table 1). Our results are in line with the previous report of formation of troglitazone reactive metabolites through oxidation by CYP3A (Kassahun et al., 2001; Tettey et al., 2001; Yamamoto et al., 2002; He et al., 2004). However, CBLs of rosiglitazone were also significantly correlated with CYP2C8 activities, and both the absolute values and the variability were greater than with troglitazone. Therefore, the risk of reactive metabolite formation alone may not explain the clinical outcomes of troglitazone hepatotoxicity.

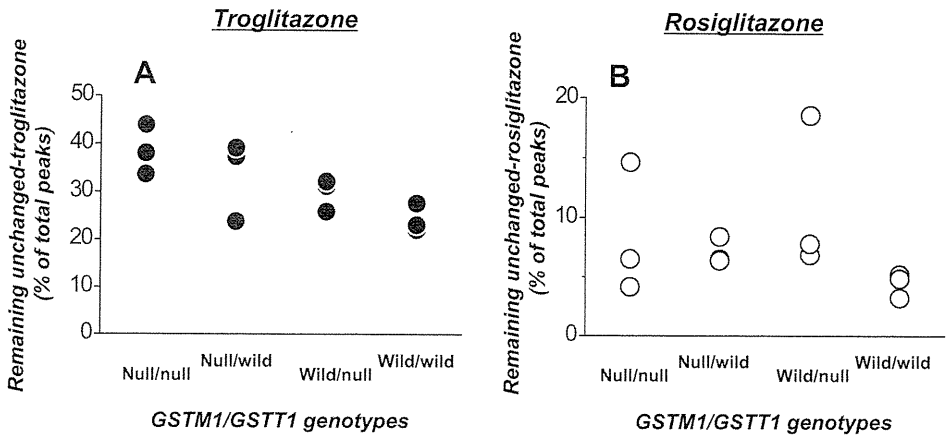

FIG. 4. Comparison of remaining unchanged drug amounts in GSTM1/GSTT1 null and wild-type hepatocytes. Radiolabeled troglitazone (A) and rosiglitazone (B) (10 μM) were incubated with 12 cryopreserved human hepatocytes genotyped for GSTM1and GSTT1 null mutations and phenotyped for P450 activity at 37°C for 8 h followed by radio-HPLC analysis of remaining unchanged troglitazone and rosiglitazone. Two-way analysis of variance results for GSTM1 genotype and for GSTT1 genotype affecting unchanged drug amounts are shown in Table 4.

DMD DRUG METABOLISM AND DISPOSITION aspet

TABLE 4

Two-way analysis of variance results for GSTM1 and GSTT1 genotypes affecting remaining unchanged drug amounts of troglitazone and rosiglitazone

Source	Troglitazone			Rosiglitazone		
	Mean Square	*F*	*p*	Mean Square	*F*	*p*
GSTM1	242.6	8.25*	0.02	0.0	0.00	0.99
GSTT1	83.9	2.85	0.13	47.7	2.54	0.15
Interaction	0.1	0.00	0.96	20.9	1.11	0.32

* Significant at $p < 0.05$.

It was reported from an earlier clinical study that GSTM1 and GSTT1 null mutations might cause ALT and AST elevation by troglitazone (Watanabe et al., 2003). Therefore, we expected that low activity of detoxification enzymes, GSTs, may be risk factors. rhGSTT1 is not commercially available, but addition of rhGSTA1 or rhGSTM1 resulted in decreased microsomal CBLs of troglitazone and rosiglitazone (Fig. 2), suggesting that GSTA1 and GSTM1 potentially have a scavenger effect on reactive metabolites. Regarding the main GST isoforms, GSTA1 and GSTP1, null mutation or polymorphism-related clinical hepatotoxicity is unknown. Thus, although rhGSTA1 also potentially had the scavenger effect, CBLs of troglitazone and rosiglitazone in GSTM1- and GSTT1-genotyped hepatocytes were investigated (Fig. 3). Concentrations studied were determined by reference to the estimated unbound maximum concentration of troglitazone in the portal vein ($C_{in,\,max,\,u}$ = 1.4 μM; calculated in Supplemental 3). The concentrations of troglitazone and rosiglitazone were determined to be 10 μM to estimate an upper limit of hepatic exposure, and thus the concentration in this assay was considered to be reasonable for evaluation of hepatotoxicity. However, CBLs of troglitazone in GSTM1/GSTT1 null hepatocytes were significantly lower than those in GSTM1/GSTT1 wild-type hepatocytes (Fig. 3A; Table 3), independent of CYP3A or CYP2C8 activities (Fig. 3C). GSTs are well known to play crucial roles in detoxification of xenobiotics by preventing the binding of reactive metabolites to cellular proteins and catalyzing the conjugation of electrophilic moieties to GSH (Hayes et al., 2005). Our results were thus contrary to the expectation that GSTs would conjugate and decrease reactive metabolites and subsequent covalent binding, suggesting that microsomal CBL measurements with exogenous rhGSTM1 do not translate to the hepatocyte system with endogenous GSTM1. These are interesting findings because of the lack of CBL differences between GSTM1/GSTT1 null and wild-type hepatocytes with rosiglitazone (Fig. 3B;

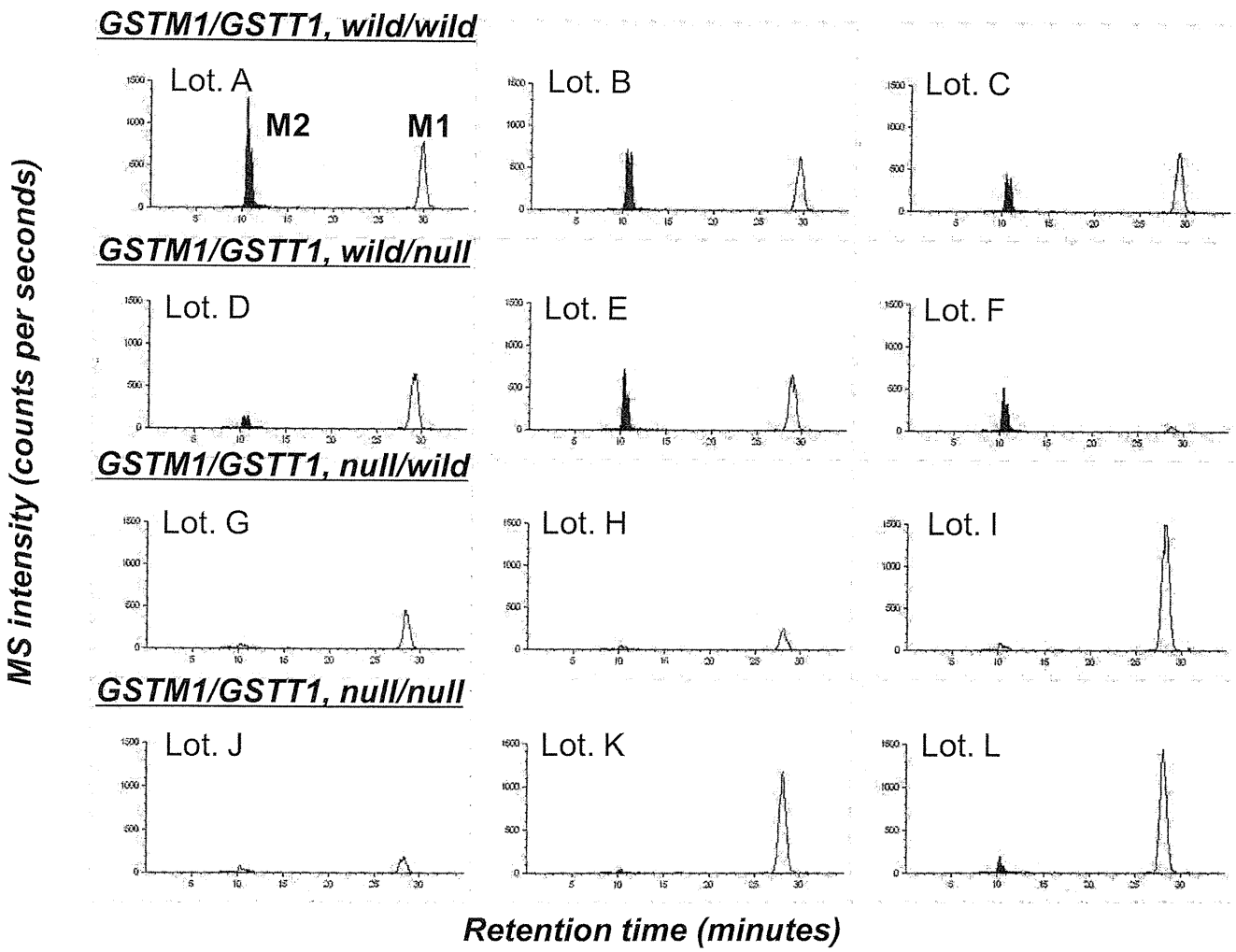

FIG. 5. LC-MS/MS chromatograms of troglitazone GSH adducts, M1 and M2, in GSTM1/GSTT1 null and wild-type hepatocytes. Filtrates after incubation of troglitazone (10 μM) with human hepatocytes genotyped for the GSTM1/GSTT1 null genotypes (lot A–C, wild/wild; lot D–F, wild/null; lot G–I, null/wild; and lot J–L, null/null) at 37°C for 8 h were applied to LC-MS/MS for detection of GSH adducts, M1 and M2, by means of the MRM method in the negative ion mode (MRM transitions: M1, $[M - H]^-$ = 745 → 272; M2, $[M - H]^-$ = 779 → 272).

DRUG METABOLISM AND DISPOSITION DMD aspet

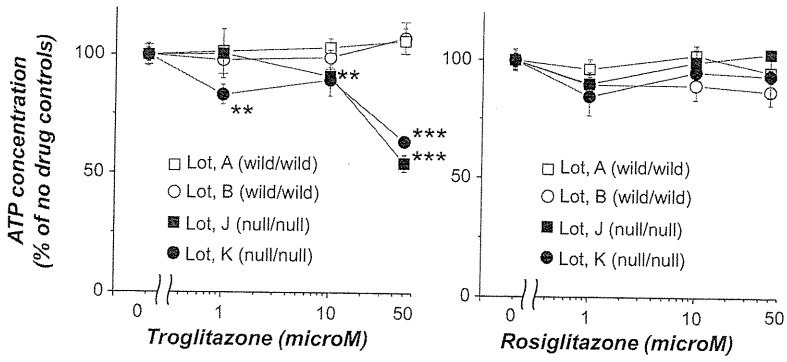

FIG. 6. Effects of GSTM1 and GSTT1 null mutations on cytotoxicity by troglitazone and rosiglitazone. Troglitazone and rosiglitazone were incubated with human cryopreserved hepatocytes genotyped for GSTM1/GSTT1 (□ and ○, wild/wild; ■ and ●, null/null) at 37°C for 2 h followed by measurement of ATP levels. Data are means ± S.D. from three assays expressed as percentages of the no drug control values. $p < 0.01$ was considered statistically significant. **, $p < 0.01$; ***, $p < 0.001$, significantly different from no drug controls.

Table 3), but unexplained, suggesting that not only CBL but also unknown factors are involved in the clinical outcomes of DILI.

In an attempt to clarify the discrepancy, metabolites of individual hepatocytes were analyzed by LC-MS/MS. Whereas M1 was found with all genotypes, M2 was scarcely obtained with GSTM1 null hepatocytes (Fig. 5). Because M2 formation is known to be catalyzed by CYP3A (Kassahun et al., 2001) and all hepatocytes used possessed a certain level of basal CYP3A activity (Table 2), it is reasonable to presume that GSTM1 is responsible for scavenging of a reactive metabolite trapped as M2. Verification of substrate selectivity for troglitazone-reactive metabolites trapped as M1 or M2 using rhGSTA1, rhGSTM1, and rhGSTP1 (Supplemental Fig. 2) indicated that M1 is formed by any GST isoforms but that M2 is formed only by rhGSTM1. It would therefore be possible to suggest that the GSH addition to a reactive metabolite to generate M1 might not be catalyzed by GSTM1, but a separate GSH addition to another metabolite to generate M2 could involve GSTM1 in hepatocytes. Specific exposure of GSTM1 null hepatocytes to the reactive metabolite trapped as M2 might have potential implications for understanding the relationship between troglitazone hepatotoxicity and GST genotypes in the clinical setting. The remaining unchanged troglitazone amounts in GSTM1 null hepatocytes were significantly higher than those in their GSTM1 wild-type counterparts (Fig. 4A; Table 4). Because troglitazone is known to be a time-dependent inhibitor of CYP3A (Kassahun et al., 2001), scavenging of reactive metabolites that bind to CYP3A protein by GSTM1 and maintaining the metabolic activity of troglitazone elimination could be a possible explanation for the discrepancy in CBL findings between exogenous rhGSTM1 and endogenous human GSTM1.

The cytotoxicity of troglitazone was investigated in the GSTM1- and GSTT1-genotyped hepatocytes. CYP3A and CYP2C8 activities affected reactive metabolite formation of troglitazone (Table 1). In addition, a combination of high CYP3A and UGT activities demonstrates association with low cytotoxicity of troglitazone, whereas low CYP3A with high SULT activity is linked to higher toxicity in human hepatocytes (Hewitt et al., 2002). However, ATP depletion was considered to be detected after treatment with troglitazone in GSTM1 and GSTT1 null hepatocytes specifically (Fig. 6) and independently of CYP2C8, CYP3A, UGT, and SULT activities (Table 2). This finding might be supportive evidence for GSTM1- and GSTT1-dependent hepatotoxicity in a clinical context, and this cytotoxicity would be expected to decrease the activities of reactive metabolite-forming enzymes and CBLs, providing another possible explanation for the discrepancy in CBL findings. Furthermore, it is interesting that GSTM1 and GSTT1 null mutation-dependent cytotoxicity was not observed for rosiglitazone.

Troglitazone sulfate, the main troglitazone metabolite eliminated into bile, shows competitive bile salt export pump inhibition with an apparent K_i value of 0.23 μM (Funk et al., 2001b). Treatment of GSTM1 and GSTT1 wild-type hepatocytes with 50 μM troglitazone did not reduce ATP levels, despite formation of a certain level of troglitazone sulfate (speculated from Supplemental Fig. 1B). Therefore, transporter inhibition might not be related to the cytotoxicity in the present study. By our system, however, the transporter activities were not investigated, and it remains to be determined whether clinical hepatotoxicity is caused by cytotoxicity or by transporter inhibition. Meanwhile, unchanged troglitazone has been reported to cause mitochondrial dysfunction (Masubuchi et al., 2006; Lim et al., 2008). Thus, our results cannot preclude the higher levels of unchanged drug in GSTM1/GSTT1 null hepatocytes (Fig. 4) being relevant to mitochondrial dysfunction. However, expression of CYP3A4 with γ-glutamylcysteine synthetase knockdown was shown to produce troglitazone cytotoxicity in a cell-based assay system (Hosomi et al., 2010, 2011), providing supportive information for our finding that high formation of reactive metabolites and low detoxification might be risk factors for troglitazone cytotoxicity.

At present, CBL is considered one of the most reliable tools to evaluate DILI (Evans et al., 2004; Nakayama et al., 2009; Usui et al., 2009). On the other hand, there are certainly some agents falsely identified as hepatotoxic by the CBL approach (Obach et al., 2008). In the case of troglitazone, CBLs of individual human hepatocytes phenotyped for P450s and genotyped for GSTs were not appropriate predictors for clinical hepatotoxicity, because the apparent inverse relationship for CBLs and cytotoxicity (and lack of P450 correlation) was observed in hepatocytes. Therefore, a cytotoxicity testing system using GSTM1- and GSTT1-genotyped hepatocytes may be more useful than a CBL measuring system using microsomes or hepatocytes. GSTM1/GSTT1 defects were found to relate to DILI with tacrine and carbamazepine in clinical studies (Simon et al., 2000; Ueda et al., 2007). It will now be necessary to investigate our evaluation system using GST-genotyped hepatocytes with more compounds.

In several recent studies, human leukocyte antigen (HLA) haplotypes were reported to be major determinants of DILI (e.g., flucloxacillin and lumiracoxib) (Daly et al., 2009; Singer et al., 2010), but the association between HLA haplotypes and troglitazone hepatotoxicity in the clinical context has not been reported. Because HLA haplotypes were not investigated in the present in vitro study, the immune idiosyncrasy in troglitazone cannot be precluded, and further study will be necessary.

In conclusion, our results demonstrate that GSTM1 and/or GSTT1 null mutations may cause higher exposure to the reactive metabolite trapped as M2 or direct cytotoxicity of troglitazone and appear to provide supportive evidence for metabolic idiosyncrasy of troglitazone hepatotoxicity in the clinical context. They are certainly informative for interpretation of mechanisms of troglitazone hepatotoxicity

and indicate that measurement of GSH adducts or cytotoxicity using GSTM1- and GSTT1-genotyped hepatocytes might offer an important in vitro system to assist in better prediction of DILI.

Acknowledgments

We acknowledge the contributions of Masashi Nakao and Dr. Tomoki Omodani in synthesizing radiolabeled compounds in-house. Appreciation is also expressed to Takeshi Takagaki for assistance with the statistical analyses and to Shinji Kimoto for assistance with the assays.

Authorship Contributions

Participated in research design: Usui, Hashizume, and Yokoi.

Conducted experiments: Usui.

Contributed new reagents or analytic tools: Usui.

Performed data analysis: Usui.

Wrote or contributed to the writing of the manuscript: Usui, Hashizume, Katsumata, Yokoi, and Komuro.

References

Arand M, Mühlbauer R, Hengstler J, Jäger E, Fuchs J, Winkler L, and Oesch F (1996) A multiplex polymerase chain reaction protocol for the simultaneous analysis of the glutathione S-transferase GSTM1 and GSTT1 polymorphisms. *Anal Biochem* **236:**184–186.

Bae MA and Song BJ (2003) Critical role of c-Jun N-terminal protein kinase activation in troglitazone-induced apoptosis of human HepG2 hepatoma cells. *Mol Pharmacol* **63:**401–408.

Daly AK, Donaldson PT, Bhatnagar P, Shen Y, Pe'er I, Floratos A, Daly MJ, Goldstein DB, John S, Nelson MR, et al. (2009) HLA-B*5701 genotype is a major determinant of drug-induced liver injury due to flucloxacillin. *Nat Genet* **41:**816–819.

Evans DC, Watt AP, Nicoll-Griffith DA, and Baillie TA (2004) Drug-protein adducts: an industry perspective on minimizing the potential for drug bioactivation in drug discovery and development. *Chem Res Toxicol* **17:**3–16.

Fujiwara T, Okuno A, Yoshioka S, and Horikoshi H (1995) Suppression of hepatic gluconeogenesis in long-term troglitazone treated diabetic KK and C57BL/KsJ-db/db mice. *Metabolism* **44:**486–490.

Funk C, Pantze M, Jehle L, Ponelle C, Scheuermann G, Lazendic M, and Gasser R (2001a) Troglitazone-induced intrahepatic cholestasis by an interference with the hepatobiliary export of bile acids in male and female rats. Correlation with the gender difference in troglitazone sulfate formation and the inhibition of the canalicular bile salt export pump (Bsep) by troglitazone and troglitazone sulfate. *Toxicology* **167:**83–98.

Funk C, Ponelle C, Scheuermann G, and Pantze M (2001b) Cholestatic potential of troglitazone as a possible factor contributing to troglitazone-induced hepatotoxicity: in vivo and in vitro interaction at the canalicular bile salt export pump (Bsep) in the rat. *Mol Pharmacol* **59:**627–635.

Gitlin N, Julie NL, Spurr CL, Lim KN, and Juarbe HM (1998) Two cases of severe clinical and histologic hepatotoxicity associated with troglitazone. *Ann Intern Med* **129:**36–38.

Hayes JD, Flanagan JU, and Jowsey IR (2005) Glutathione transferases. *Annu Rev Pharmacol Toxicol* **45:**51–88.

He K, Talaat RE, Pool WF, Reily MD, Reed JE, Bridges AJ, and Woolf TF (2004) Metabolic activation of troglitazone: identification of a reactive metabolite and mechanisms involved. *Drug Metab Dispos* **32:**639–646.

Hewitt NJ, Lloyd S, Hayden M, Butler R, Sakai Y, Springer R, Fackett A, and Li AP (2002) Correlation between troglitazone cytotoxicity and drug metabolic enzyme activities in cryopreserved human hepatocytes. *Chem Biol Interact* **142:**73–82.

Hosomi H, Akai S, Minami K, Yoshikawa Y, Fukami T, Nakajima M, and Yokoi T (2010) An in vitro drug-induced hepatotoxicity screening system using CYP3A4-expressing and γ-glutamylcysteine synthetase knockdown cells. *Toxicol In Vitro* **24:**1032–1038.

Hosomi H, Fukami T, Iwamura A, Nakajima M, and Yokoi T (2011) Development of a highly sensitive cytotoxicity assay system for CYP3A4-mediated metabolic activation. *Drug Metab Dispos* doi:10.1124/dmd.110.037077.

Isley WL (2003) Hepatotoxicity of thiazolidinediones. *Expert Opin Drug Saf* **2:**581–586.

Kassahun K, Pearson PG, Tang W, McIntosh I, Leung K, Elmore C, Dean D, Wang R, Doss G, and Baillie TA (2001) Studies on the metabolism of troglitazone to reactive intermediates *in vitro* and *in vivo*. Evidence for novel biotransformation pathways involving quinone methide formation and thiazolidinedione ring scission. *Chem Res Toxicol* **14:**62–70.

Lim PL, Liu J, Go ML, and Boelsterli UA (2008) The mitochondrial superoxide/thioredoxin-2/Ask1 signaling pathway is critically involved in troglitazone-induced cell injury to human hepatocytes. *Toxicol Sci* **101:**341–349.

Masubuchi Y, Kano S, and Horie T (2006) Mitochondrial permeability transition as a potential determinant of hepatotoxicity of antidiabetic thiazolidinediones. *Toxicology* **222:**233–239.

Nakayama S, Atsumi R, Takakusa H, Kobayashi Y, Kurihara A, Nagai Y, Nakai D, and Okazaki O (2009) A zone classification system for risk assessment of idiosyncratic drug toxicity using daily dose and covalent binding. *Drug Metab Dispos* **37:**1970–1977.

Nozawa T, Sugiura S, Nakajima M, Goto A, Yokoi T, Nezu J, Tsuji A, and Tamai I (2004) Involvement of organic anion transporting polypeptides in the transport of troglitazone sulfate: implications for understanding troglitazone hepatotoxicity. *Drug Metab Dispos* **32:**291–294.

Obach RS, Kalgutkar AS, Soglia JR, and Zhao SX (2008) Can in vitro metabolism-dependent covalent binding data in liver microsomes distinguish hepatotoxic from nonhepatotoxic drugs? An analysis of 18 drugs with consideration of intrinsic clearance and daily dose. *Chem Res Toxicol* **21:**1814–1822.

Russmann S, Jetter A, and Kullak-Ublick GA (2010) Pharmacogenetics of drug-induced liver injury. *Hepatology* **52:**748–761.

Saha S, New LS, Ho HK, Chui WK, and Chan EC (2010) Direct toxicity effects of sulfo-conjugated troglitazone on human hepatocytes. *Toxicol Lett* **195:**135–141.

Shiau CW, Yang CC, Kulp SK, Chen KF, Chen CS, Huang JW, and Chen CS (2005) Thiazolidenediones mediate apoptosis in prostate cancer cells in part through inhibition of Bcl-xL/Bcl-2 functions independently of PPARγ. *Cancer Res* **65:**1561–1569.

Shibuya A, Watanabe M, Fujita Y, Saigenji K, Kuwao S, Takahashi H, and Takeuchi H (1998) An autopsy case of troglitazone-induced fulminant hepatitis. *Diabetes Care* **21:**2140–2143.

Sigrist S, Bedoucha M, and Boelsterli UA (2000) Down-regulation by troglitazone of hepatic tumor necrosis factor-α and interleukin-6 mRNA expression in a murine model of non-insulin-dependent diabetes. *Biochem Pharmacol* **60:**67–75.

Simon T, Becquemont L, Mary-Krause M, de Waziers I, Beaune P, Funck-Brentano C, and Jaillon P (2000) Combined glutathione-S-transferase M1 and T1 genetic polymorphism and tacrine hepatotoxicity. *Clin Pharmacol Ther* **67:**432–437.

Singer JB, Lewitzky S, Leroy E, Yang F, Zhao X, Klickstein L, Wright TM, Meyer J, and Paulding CA (2010) A genome-wide study identifies HLA alleles associated with lumiracoxib-related liver injury. *Nat Genet* **42:**711–714.

Sparano N and Seaton TL (1998) Troglitazone in type II diabetes mellitus. *Pharmacotherapy* **18:**539–548.

Tettey JN, Maggs JL, Rapeport WG, Pirmohamed M, and Park BK (2001) Enzyme-induction dependent bioactivation of troglitazone and troglitazone quinone *in vivo*. *Chem Res Toxicol* **14:**965–974.

Ueda K, Ishitsu T, Seo T, Ueda N, Murata T, Hori M, and Nakagawa K (2007) Glutathione S-transferase M1 null genotype as a risk factor for carbamazepine-induced mild hepatotoxicity. *Pharmacogenomics* **8:**435–442.

Uetrecht J (2009) Immune-mediated adverse drug reactions. *Chem Res Toxicol* **22:**24–34.

Usui T, Mise M, Hashizume T, Yabuki M, and Komuro S (2009) Evaluation of the potential for drug-induced liver injury based on in vitro covalent binding to human liver proteins. *Drug Metab Dispos* **37:**2383–2392.

Walgren JL, Mitchell MD, and Thompson DC (2005) Role of metabolism in drug-induced idiosyncratic hepatotoxicity. *Crit Rev Toxicol* **35:**325–361.

Watanabe I, Tomita A, Shimizu M, Sugawara M, Yasumo H, Koishi R, Takahashi T, Miyoshi K, Nakamura K, Izumi T, et al. (2003) A study to survey susceptible genetic factors responsible for troglitazone-associated hepatotoxicity in Japanese patients with type 2 diabetes mellitus. *Clin Pharmacol Ther* **73:**435–455.

Watanabe T, Ohashi Y, Yasuda M, Takaoka M, Furukawa T, Yamato T, Sanbuissho A, and Manabe S (1999) Was it possible to predict liver dysfunction caused by troglitazone during the nonclinical safety studies? *Iyakuhin Kenkyu* **30:**537–546.

Yamamoto Y, Yamazaki H, Ikeda T, Watanabe T, Iwabuchi H, Nakajima M, and Yokoi T (2002) Formation of a novel quinone epoxide metabolite of troglitazone with cytotoxicity to HepG2 cells. *Drug Metab Dispos* **30:**155–160.

Address correspondence to: Toru Usui, Pharmacokinetics Research Laboratories, Dainippon Sumitomo Pharma Co., Ltd., 3-1-98, Kasugade-naka, Konohana-ku, Osaka, 554-0022, Japan. E-mail: toru-usui@ds-pharma.co.jp

Supplemental Material can be found at:
http://dmd.aspetjournals.org/content/suppl/2011/05/03/dmd.110.037077.DC1.html

0090-9556/11/3908-1388–1395$25.00
DRUG METABOLISM AND DISPOSITION
Vol. 39, No. 8
37077/3701350
Printed in U.S.A.

DMD 39:1388–1395, 2011

Development of a Highly Sensitive Cytotoxicity Assay System for CYP3A4-Mediated Metabolic Activation[S]

Hiroko Hosomi, Tatsuki Fukami, Atsushi Iwamura, Miki Nakajima, and Tsuyoshi Yokoi

Drug Metabolism and Toxicology, Faculty of Pharmaceutical Sciences, Kanazawa University, Kakuma-machi, Kanazawa, Japan

Received November 4, 2010; accepted May 3, 2011

ABSTRACT:

Drug-induced hepatotoxicity, which is a rare but serious adverse reaction to a large number of pharmaceutical drugs, is sometimes associated with reactive metabolites produced by drug-metabolizing enzymes. In the present study, we constructed a cell-based system to evaluate the cytotoxicity of reactive metabolites produced by CYP3A4 using human hepatoma cells infected with an adenovirus vector expressing human CYP3A4 (AdCYP3A4). When seven hepatoma cell lines (HepG2, Hep3B, HLE, HLF, Huh6, Huh7, and Fa2N4 cells) were infected with AdCYP3A4, HepG2 cells showed the highest CYP3A4 protein expression and testosterone 6β-hydroxylase activity (670 pmol · min^{-1} · mg^{-1}). With the use of AdCYP3A4-infected HepG2 cells, the cytotoxicities of 23 drugs were evaluated by the 2-(2-methoxy-4-nitrophenyl)-3-(4-nitrophenyl)-5-(2,4-disulfophenyl)-2*H*-tetrazolium monosodium salt assay, and the cell viability when treated with 11 drugs (amiodarone, desipramine, felbamate, isoniazid, labetalol, leflunomide, nefazodone, nitrofurantoin, tacrine, terbinafine, and tolcapone) was significantly decreased. Moreover, the transfection of siRNA for nuclear factor erythroid 2-related factor 2 (Nrf2) to decrease the cellular expression level of Nrf2 exacerbated the cytotoxicity of some drugs (troglitazone, flutamide, acetaminophen, clozapine, terbinafine, and desipramine), suggesting that the genes regulated by Nrf2 are associated with the detoxification of the cytotoxicities mediated by CYP3A4. We constructed a highly sensitive cell-based system to detect the drug-induced cytotoxicity mediated by CYP3A4. This system would be beneficial in preclinical screening in drug development and increase our understanding of the drug-induced cytotoxicity associated with CYP3A4.

Introduction

Drug-induced hepatotoxicity is a rare but serious adverse reaction to a large number of pharmaceutical drugs (Boelsterli and Lim, 2007). One of the mechanisms suggested for the drug-induced hepatotoxicity is associated with reactive metabolites produced by drug-metabolizing enzymes (Guengerich and MacDonald, 2007). For example, if the reactive metabolites covalently bind to intracellular proteins, cellular dysfunctions are apparently produced, resulting in the loss of ionic gradients, a decline in ATP levels, actin disruption, cell swelling, and cell rupture (Beaune et al., 1987; Yun et al., 1993). Although drug-induced hepatotoxicity can be evaluated using laboratory animal models, species differences in drug-metabolizing enzymes or other factors between humans and laboratory animals have made the prediction of drug-induced cytotoxicity difficult. Several studies used human hepatocytes to evaluate the drug-induced cytotoxicity mediated by drug-metabolizing enzymes (Li et al., 1999; Gómez-Lechón et al., 2003), but this approach is often not applicable because of the poor availability of human liver, the high cost, the significant variability among human hepatocyte preparations, and, in particular, the unstable enzyme activities of human hepatocytes.

To date, several systems for evaluating drug-induced cytotoxicity mediated by drug-metabolizing enzymes have been developed. Yoshitomi et al. (2001) used HepG2 cells stably expressing human cytochrome P450 (P450) enzymes, and the viabilities of the cells expressing CYP1A2, CYP2E1, and CYP3A4 were decreased in an acetaminophen concentration-dependent manner. Vignati et al. (2005) demonstrated, using HepG2 cells transiently transfected with CYP3A4, that reactive metabolites of various hepatotoxic drugs such as albendazole, flutamide, and troglitazone were produced by CYP3A4. Our previous study showed that benzodiazepines such as flunitrazepam and nimetazepam were metabolically activated by CYP3A4 by coincubation with HepG2 cells and CYP3A4 Supersomes (Mizuno et al., 2009). Thus, several in vitro studies demonstrated that P450 enzymes, especially CYP3A4, are involved in the cytotoxicities of various kinds of drugs. However, transfection of P450 expression plasmids into cells generally could not achieve high expression of P450 enzymes. In addition, many studies used cells with GSH levels decreased by treatment with L-buthionine sulfoximine to easily detect the cytotoxicity. Indeed, the GSH-conjugating process is responsible for the detoxification of reactive metabolites, but we considered that cells with decreased nuclear factor erythroid 2-related

This work was supported by Health and Labor Science Research Grants from the Ministry of Health, Labor, and Welfare of Japan [Grant H20-BIO-G001].

Article, publication date, and citation information can be found at http://dmd.aspetjournals.org.

doi:10.1124/dmd.110.037077.

[S] The online version of this article (available at http://dmd.aspetjournals.org) contains supplemental material.

ABBREVIATIONS: P450, cytochrome P450; Nrf2, nuclear factor erythroid 2-related factor 2; GCLC, glutamate-cysteine ligase, catalytic subunit; GCLM, glutamate-cysteine ligase, modifier subunit; 3-HAA, 3-hydroxyacetanilide; RT, reverse transcription; PCR, polymerase chain reaction; GAPDH, glyceraldehyde-3-phosphate dehydrogenase; MOI, multiplicity of infection; WST-8, 2-(2-methoxy-4-nitrophenyl)-3-(4-nitrophenyl)-5-(2,4-disulfophenyl)-2*H*-tetrazolium monosodium salt; TBF-A, 7,7-dimethylhept-2-ene-4-ynal.

factor 2 (Nrf2) levels would also be useful to sensitively detect the cytotoxicity, because Nrf2 is a transcription factor that acts as a main regulator for the up-regulation of a group of genes coding antioxidant proteins and phase II drug-metabolizing enzymes, such as NADPH-quinone oxidoreductase 1, heme oxygenase-1, and glutamate-cysteine ligase, catalytic subunit (GCLC) and modifier subunit (GCLM) (Thimmulappa et al., 2002; Balogun et al., 2003; Nioi et al., 2003). In fact, it has been reported that Nrf2 knockout mice had increased susceptibility to acetaminophen (Chan et al., 2001).

In a previous study, we established an adenovirus that could overexpress human CYP3A4 (AdCYP3A4) (Hosomi et al., 2010). In this study, we developed a highly sensitive in vitro cell-based assay system using AdCYP3A4 and investigated whether CYP3A4 is involved in the cytotoxicity of 23 drugs that are known to cause hepatotoxicity in humans. In addition, we investigated whether treatment with siNrf2 exacerbates the drug-induced cytotoxicity mediated by CYP3A4.

Materials and Methods

Chemicals and Reagents. Acetaminophen, allopurinol, clozapine, corticosterone, cyclizine, dantrolene sodium, desipramine, disulfiram, erythromycin, felbamate, 3-hydroxyacetanilide (3-HAA), maprotiline, nefazodone, nilutamide, rosiglitazone, sulindac, tacrine, terbinafine, testosterone, tolcapone, troglitazone, and zafirlukast were obtained from Wako Pure Chemicals (Osaka, Japan). Flutamide, 6β-hydroxytestosterone, isoniazid, labetalol, and nitrofurantoin were obtained from Sigma-Aldrich (St. Louis, MO). Amiodarone and leflunomide were obtained from LKT Labs (St. Paul, MN) and Enzo Life Sciences, Inc. (Farmingdale, NY), respectively. ReverTra Ace (Moloney murine leukemia virus reverse transcriptase RNaseH Minus) was from Toyobo (Tokyo, Japan). The Adenovirus Expression Vector Kit (Dual Version), RNAiso, random hexamer, and SYBR Premix Ex Taq were obtained from Takara (Shiga, Japan). The QuickTiter Adenovirus Titer Immunoassay Kit was from Cell Biolabs (Tokyo, Japan). Stealth Select RNAi for Nrf2 (siNrf2) (accession number NM_006164) and Stealth RNAi Negative Control Medium GC Duplex #2 (siScramble), Lipofectamine RNAiMAX Reagent, and Lipofectamine 2000 were obtained from Invitrogen (Carlsbad, CA). Dulbecco's modified Eagle's medium was from Nissui Pharmaceutical (Tokyo, Japan). MFE support media (serum-free) was from MultiCell Technologies (Lincoln, RI). All primers were commercially synthesized at Hokkaido System Sciences (Sapporo, Japan). Other chemicals were of analytical or the highest grade commercially available.

Cell Culture. The 293 and HepG2 cells were obtained from American Type Culture Collection (Manassas, VA). The HLE and Huh7 cells were obtained from Japan Collection of Research Biosources (Tokyo, Japan) and RIKEN BioResource Center (Ibaraki, Japan), respectively. The Fa2N4 cells were obtained from MultiCell Technologies. The Hep3B, Huh6, and HLF cells were kindly provided by Dr. Shuichi Kaneko (Kanazawa University, Kanazawa, Japan). The 293, HepG2, Hep3B, HLE, HLF, Huh6, and Huh7 cells were maintained in Dulbecco's modified Eagle's medium containing 10% fetal bovine serum (Invitrogen), 3% glutamine, 16% sodium bicarbonate, and 0.1 mM nonessential amino acids (Invitrogen) in a 5% CO_2 atmosphere at 37°C. Fa2N4 cells were grown on collagen-coated flasks and maintained in MFE support media containing 10% fetal bovine serum. When adenovirus was used to infect the cell lines, a medium containing 5% fetal bovine serum was used.

siRNA Treatment. HepG2 cells were transfected with siNrf2 or siScramble by Lipofectamine RNAiMAX Reagent. According to the manufacturer's protocol, RNAi duplex-Lipofectamine RNAiMAX complexes were prepared and added to each well before the HepG2 cells were seeded (2.0×10^4 cells/well). The concentrations of siNrf2 and siScramble were 10 nM.

Total RNA Preparation from Hepatoma Cells and Real-Time RT-PCR. Total RNA from hepatoma cells was isolated using RNAiso. The RT procedure was described previously (Nakajima et al., 2006). Human Nrf2 was quantified by real-time RT-PCR using the Smart Cycler (Cepheid, Sunnyvale, CA). The sequences of sense and antisense primers were 5′-CAACACACGGTCCACAGC-3′ and 5′-CAATATTAAGACACTGTAACTC-3′, respectively. A 1-μl portion of the reverse-transcribed mixture was added to a PCR mixture containing 10 pmol of sense and antisense primers and 12.5 μl of SYBR Premix Ex Taq solution in a final volume of 25 μl. The PCR conditions were as follows: after an initial denaturation at 95°C for 30 s, the amplification was performed by denaturation at 94°C for 6 s and annealing and extension at 64°C for 20 s for 45 cycles. Human glyceraldehyde 3-phosphate dehydrogenase (GAPDH) mRNA was also quantified as described previously (Tsuchiya et al., 2004). The expression level of Nrf2 mRNA was normalized with the GAPDH mRNA level.

Nrf2 Protein Level. The Nrf2 protein level was measured as described previously (Nakamura et al., 2008) with slight modifications. Cell lysates (30 μg) were separated on 7.5% polyacrylamide gel electrophoresis and electrotransferred onto Immobilon-P polyvinylidene difluoride membrane (Millipore Corporation, Billerica, MA). The membranes were probed with polyclonal rabbit anti-Nrf2 antibody (H-300) (Santa Cruz Biotechnology, Inc., Santa Cruz, CA), polyclonal rabbit anti-human GAPDH polyclonal antibodies (Sekisui Medical, Tokyo, Japan), and anti-rabbit IgG-conjugated IRDye680, and an Odyssey infrared imaging system (LI-COR Biosciences, Lincoln, NE) were used for the detection. The relative expression level was quantified using ImageQuant TL Image Analysis software (GE Healthcare, Little Chalfont, Buckinghamshire, UK).

CYP3A4 Enzyme Activity. AdCYP3A4 was constructed in our previous study (Hosomi et al., 2010). HepG2 cells (3×10^5 cells/well) were seeded in 12-well plates. After a 24-h incubation, the cells were infected with AdCYP3A4 for 48 h at a multiplicity of infection (MOI) of 10 (MOI 10). Then, after a 1-h incubation with 100 μM testosterone, the concentration of 6β-hydroxytestosterone, a metabolite of testosterone by CYP3A4, in the medium was measured as described previously (Hosomi et al., 2010).

Cytotoxicity Assay. HepG2 cells (2.0×10^4 cells/well) were seeded in 96-well plates and, if necessary, were treated with siNrf2 or siScramble as described above. After a 24-h incubation, the cells were infected with AdCYP3A4 or the recombinant adenovirus vector expressing green fluorescence protein (AdGFP) constructed in our previous study (Hosomi et al., 2010). The titers of AdCYP3A4 and AdGFP were 6.4×10^8 and 2.1×10^8 plaque forming units/ml, respectively. Forty-eight hours after infection at MOI 10, the cells were treated with various drugs for 24 h. After incubation with the drugs, cell viability was quantified by 2-(2-methoxy-4-nitrophenyl)-3-(4-nitrophenyl)-5-(2,4-disulfophenyl)-2*H*-tetrazolium monosodium salt (WST-8) and ATP assays according to the manufacturer's protocol. The WST-8 assay, which is a modified 3-(4,5-dimethylthiazol-2-yl)2,5-diphenyl tetrazolium bromide assay, was performed using Cell Counting Kit-8 (Wako Pure Chemicals). After incubation with the drugs, Cell Counting Kit-8 reagent was added, and absorbance of WST-8 formazan was measured at 405 nm. The ATP assay was performed using a CellTiter-Glo Luminescent Cell Viability Assay (Promega, Madison, WI). After incubation with the drugs, CellTiter-Glo Reagent was added, and the generation of luminescent signals was recorded by using a 1420 ARVO MX luminometer (PerkinElmer Life and Analytical Sciences-Wallac Oy, Turku, Finland).

Statistical Analyses. Comparisons of two and several groups were made with a unpaired, two-tailed Student's *t* test and Dunnett's test, respectively. $P < 0.05$ was considered statistically significant.

Results

CYP3A4 Enzyme Activity in Various Hepatoma Cell Lines Infected with AdCYP3A4. To determine which hepatoma cell line is suitable for the evaluation of drug-induced cytotoxicity mediated by CYP3A4, seven hepatoma cell lines (HepG2, Hep3B, HLE, HLF, Huh6, Huh7, and Fa2N4 cells) were infected with AdCYP3A4 at MOI 10, and the testosterone 6β-hydroxylase activity was measured at a concentration of 100 μM (Fig. 1). Among these cell lines, HepG2 cells showed the highest enzyme activity (670 pmol · min^{-1} · mg $protein^{-1}$). Huh7 cells also showed moderate enzyme activity (233 pmol · min^{-1} · mg $protein^{-1}$), but the other cells showed activity at less than 100 pmol · min^{-1} · mg $protein^{-1}$. From this result, HepG2 cells were used in the subsequent studies.

Cytotoxic Effects of CYP3A4 on Cell Viability of HepG2 Cells. To investigate whether CYP3A4 is associated with the cytotoxicity of 23 drugs (acetaminophen, allopurinol, amiodarone, clozapine, cycliz-

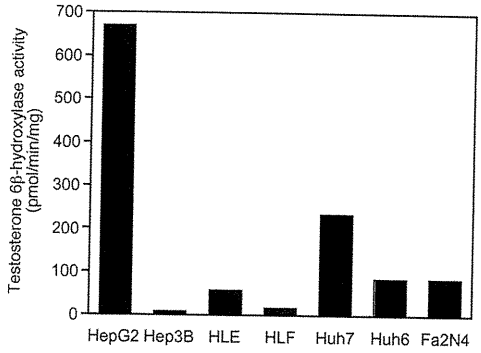

FIG. 1. CYP3A4 enzyme activity in various cell lines infected with AdCYP3A4. Cells were infected with AdCYP3A4 at MOI 10 for 48 h, and the testosterone 6β-hydroxylase activity was measured as described under *Materials and Methods*. Data are the means of two independent experiments.

ine, dantrolene, desipramine, disulfiram, erythromycin, felbamate, flutamide, isoniazid, labetalol, leflunomide, maprotiline, nefazodone, nitrofurantoin, sulindac, tacrine, terbinafine, tolcapone, troglitazone, and zafirlukast), HepG2 cells infected with AdCYP3A4 at MOI 10 for 48 h were treated with the drugs for 24 h (Fig. 2). As a negative control, AdGFP was infected at MOI 10. The cytotoxicity assay was performed at the concentrations less than the concentration that showed the typical decreased cell viability by the parent drugs. However, the range of concentrations was at least 30 times the clinically efficacious concentration or 100 μM according to a previous report (O'Brien et al., 2006). Cytotoxicity was evaluated by the WST-8 assay (Fig. 2), which showed that the viabilities of the cells infected with AdCYP3A4 were significantly decreased compared with that of those infected with AdGFP when treated with amiodarone (10 and 25 μM), desipramine (10 and 25 μM), disulfiram (25–100 μM), isoniazid (50 and 100 μM), leflunomide (100 μM), nefazodone (25 μM), tacrine (100 μM), terbinafine (10–50 μM), or tolcapone (20 and 50 μM). However, the other drugs did not affect the cell viability by the overexpression of CYP3A4 in the HepG2 cells.

Cytotoxic Effects of Knockdown of Nrf2 Expression on Cell Viability of HepG2 Cells. Nrf2 is a transcription factor that acts as an important regulator of the up-regulation of a group of genes coding antioxidant proteins and phase II drug-metabolizing enzymes, such as NADPH-quinone oxidoreductase, heme oxidase-1, and GCLC. Therefore, decreased Nrf2 levels in the cells may enhance the drug-induced cytotoxicity caused by CYP3A4. In this study, the drug-induced cytotoxicity mediated by CYP3A4 was investigated using AdCYP3A4-infected HepG2 cells transfected with siNrf2. The expression level of Nrf2 mRNA in HepG2 cells treated with siNrf2 for 72 and 96 h was lower than 90% of that of cells treated with siScramble (Fig. 3A). The expression level of Nrf2 protein in HepG2 cells treated with siNrf2 was also 55 to 75% lower than that of cells treated with siScramble (Fig. 3B). The effect of siNrf2 on the expression levels of Nrf2 mRNA and protein was not different between the treatments with AdGFP and AdCYP3A4. In addition, the HepG2 cell lysate treated with siNrf2 showed testosterone 6β-hydroxylase activity (781 ± 47 pmol · min^{-1} · mg $protein^{-1}$) similar to that of cell lysate treated with siScramble (720 ± 40 pmol · min^{-1} · mg $protein^{-1}$) (Fig. 3C). Therefore, it was confirmed that the decreased level of Nrf2 expression did not affect the testosterone 6β-hydroxylase activity.

With the use of HepG2 cells, the drug-induced cytotoxicity was investigated (Fig. 4). As a negative control against siNrf2, siScramble was transfected to HepG2 cells. Four drugs (troglitazone, flutamide, acetaminophen, and clozapine) that did not show cytotoxicity in the presence of CYP3A4 in the previous analysis (Fig. 2) and two drugs (desipramine and terbinafine) that showed cytotoxicity (Fig. 2) were investigated. In the WST-8 assay, the viabilities of AdCYP3A4-infected cells with siNrf2 were significantly decreased compared with those with siScramble for treatment with troglitazone (25 and 50 μM), flutamide (10–50 μM), acetaminophen (2.5–20 mM), clozapine (25–50 μM), desipramine (10 and 25 μM), or terbinafine (10 and 25 μM) (Fig. 4A). The ATP assay showed results similar to those of the WST-8 assay, although the magnitude of the difference in cell viability between cells with siNrf2 and those with siScramble was smaller (Fig. 4B). Thus, these results suggested that AdCYP3A4-infected HepG2 cells with decreased levels of Nrf2 were useful to evaluate the drug-induced cytotoxicity mediated by CYP3A4.

To investigate whether any drugs may affect the viability of cells with decreased levels of Nrf2, we examined the changes in cell viability by treatment with rosiglitazone, nilutamide, and 3-HAA, which have been reported to show a lower risk of hepatotoxicity but have structures similar to troglitazone, flutamide, and acetaminophen (Supplemental Fig. 1). However, rosiglitazone, nilutamide, and 3-HAA did not show decreased cell viability even when the Nrf2 level in cells was decreased. This result was consistent with the fact that these drugs are not likely to be associated with CYP3A4-mediated hepatotoxicity.

Discussion

Drug-induced hepatotoxicity is a rare but serious adverse reaction to a large number of pharmaceutical drugs (Boelsterli and Lim, 2007). Because drug-induced hepatotoxicity is sometimes associated with reactive metabolites produced by drug-metabolizing enzymes (Guengerich and MacDonald, 2007), it would be ideal to be able to predict the hepatotoxicity mediated by these enzymes using an in vitro system. In the present study, we constructed a highly sensitive cell-based system to detect the cytotoxicity of drugs using HepG2 cells expressing CYP3A4, which is a predominant P450 isoform in human liver that is responsible for more than 50% of drug metabolism (Guengerich, 2008).

In general, infection of cells with a recombinant adenovirus can lead to high expression of specific genes of interest. In our previous study, we introduced the overexpression of CYP3A4 protein in rat hepatoma cells, H4IIE cells, by the infection of AdCYP3A4 (Hosomi et al., 2010). Likewise, in this study, seven human hepatoma cell lines were infected with AdCYP3A4, and the testosterone 6β-hydroxylase activity was measured. Among them, HepG2 cells showed the highest enzyme activity (Fig. 1). This result might reflect the fact that HepG2 cells express high endogenous levels of NADPH-P450 reductase and cytochrome b_5 (Aoyama et al., 1990) in addition to the high efficiency of infection. The testosterone 6β-hydroxylase activity of AdCYP3A4-infected HepG2 cells (670 pmol · min^{-1} · mg $protein^{-1}$ at 100 μM testosterone) was more than 2.5-fold higher than the V_{max} values of the activity in human hepatocytes reported by Donato et al. (1995) and Gómez-Lechón et al. (2001) (177 ± 98 and 253 ± 110 pmol · min^{-1} · mg $protein^{-1}$, respectively). Given the large interindividual variability in CYP3A4 protein expression (a 32-fold variability) (Westlind-Johnsson et al., 2003), the cells used in this study would mimic human hepatocytes that exhibit the highest CYP3A4 enzyme activity.

In this study, we investigated the CYP3A4-mediated cytotoxicity of 23 drugs that are known to cause hepatotoxicity in humans (Xu et al., 2008). The viability of cells infected with AdCYP3A4 was significantly decreased by treatment with amiodarone, desipramine, disulfiram, isoniazid, leflunomide, nefazodone, nitrofurantoin, tacrine, terbinafine, and tolcapone compared with those infected with AdGFP. It has already been reported that the hepatotoxicity of some drugs is associated with the metabolic activation mediated by CYP3A4. The major metabolite of amiodarone, desethylamiodarone, was reported to

DRUG METABOLISM AND DISPOSITION DMD aspet

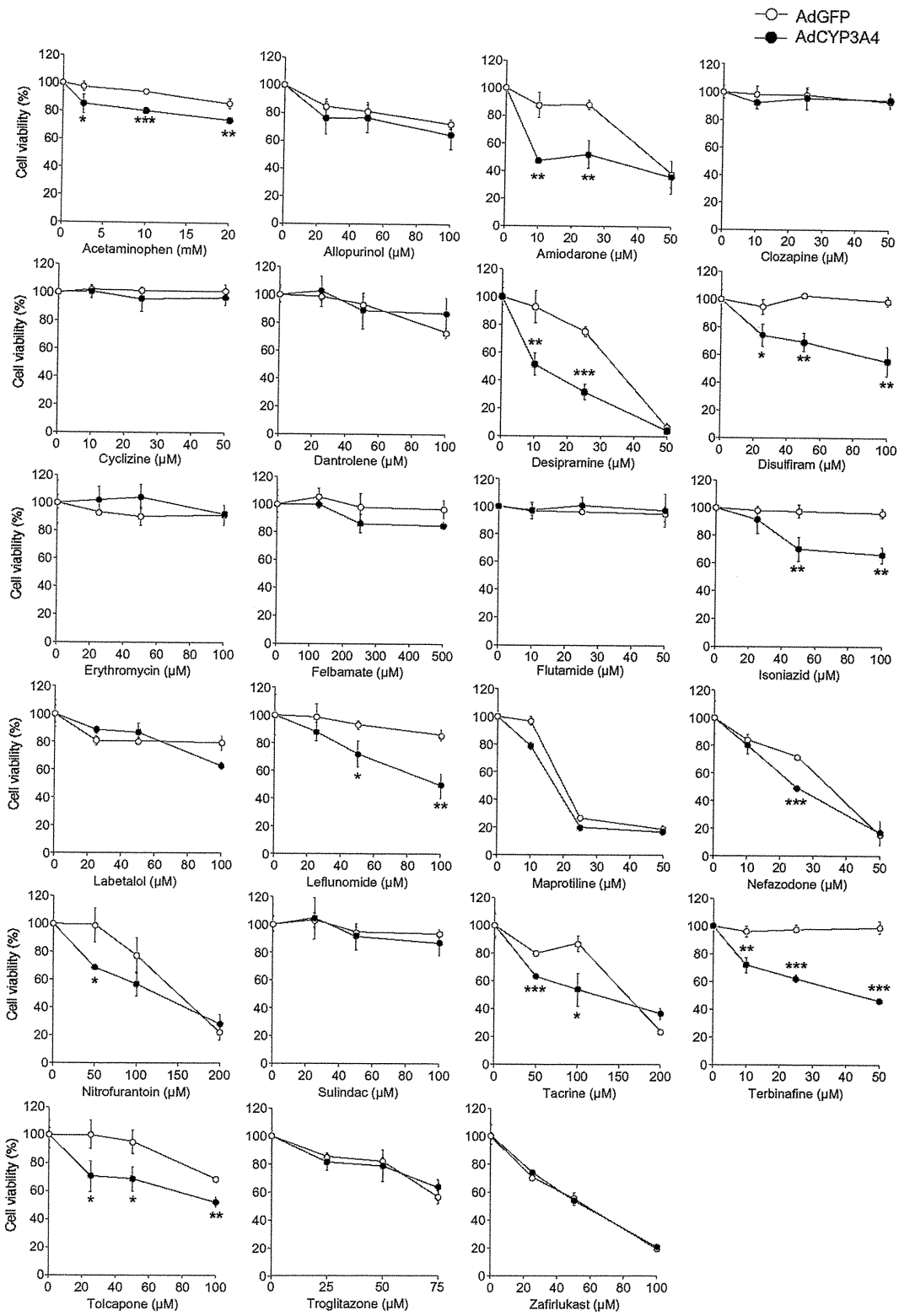

FIG. 2. Cytotoxic effects of CYP3A4 expression on cell viability of HepG2 cells treated with various drugs. HepG2 cells were infected with AdCYP3A4 (●) or AdGFP (○) at MOI 10 for 48 h and treated with 23 drugs for 24 h. Cell viability was measured by the WST-8 assay. Each point represents the mean ± S.D. (n = 3). *, $P < 0.05$; **, $P < 0.01$; ***, $P < 0.001$, compared with the AdGFP group at each concentration of the drug.

cause cytotoxicity in HepG2 cells and rat hepatocytes at lower concentrations than the parent drug amiodarone (McCarthy et al., 2004). Desethylamiodarone is produced mainly by CYP3A4 and by CYP2C8 in humans (Ohyama et al., 2000). Erythromycin-associated hepatic injury is usually cholestatic and may mimic obstructive jaundice (Klatskin, 1975). Although CYP3A4 is involved in erythromycin

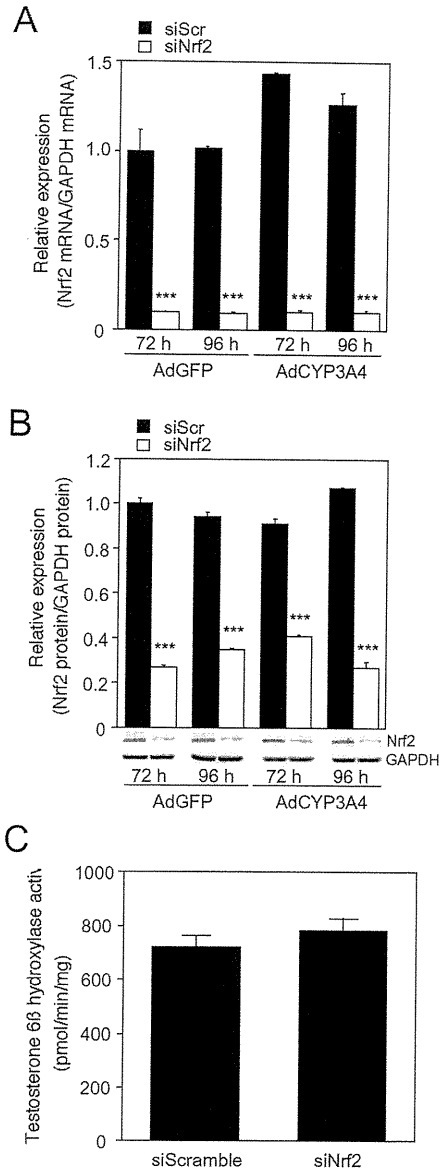

FIG. 3. Expression level of Nrf2 mRNA (A) and protein (B) and testosterone 6β-hydroxylase activity (C) in AdCYP3A4-infected HepG2 cells with siNrf2. After HepG2 cells were transfected with siNrf2 or siScramble at 10 nM followed by the infection with AdCYP3A4 or AdGFP at MOI 10 for 48 h, the expression level of Nrf2 mRNA and protein and testosterone 6β-hydroxylase activity were measured as described under *Materials and Methods*. Each column represents the means ± S.D. ($n = 3$). ***, $P < 0.001$ compared with AdCYP3A4-infected cells with siScramble.

metabolism and the substrate to which erythromycin binds has been identified (Watkins, 1992), it has no demonstrated relevance to erythromycin metabolism-associated hepatic injury. Nefazodone is metabolized to hydroxynefazodone, followed by the formation of quinone-imine and 2-chloro-1,4-benzoquinone, which would be associated with the hepatotoxicity, in human liver microsomes. These reactions are mediated by CYP3A4 (Kalgutkar et al., 2005). Terbinafine is mainly metabolized to *N*-demethylterbinafine, 7,7-dimethylhept-2-ene-4-ynal (TBF-A), and several hydroxy forms in human liver. Among them, TBF-A, which is produced by CYP3A4, was reported to cause terbinafine-induced hepatotoxicity (Iverson and Uetrecht, 2001). However, no association of CYP3A4 with desipramine-, disulfiram-, isoniazid-, leflunomide-, nitrofurantoin-, and tolcapone-induced hepatotoxicity has been reported, although most of these drugs appeared to be metabolically activated by P450 enzymes. For example, CYP1A2 is reported to be associated with the formation of iminoquinone from tacrine and tolcapone (Balson et al., 1995; Smith et al., 2003). Furthermore, CYP2E1 is considered to be associated with isoniazid-induced hepatotoxicity by metabolizing acetylhydrazine, one of the metabolites of isoniazid, to *N*-acetylhydrazine (Huang et al., 2003). Further studies on the involvement of CYP3A4 in the metabolic activation of these drugs are needed. Although pharmacological drug interactions were reported in cyclizine, a metabolic activation pathway would not be involved.

Nitroaromatic drugs such as tacrine and nitrofurantoin have been associated with liver injury (Boelsterli et al., 2006). In the reductive pathways from nitro to the fully reduced amine catalyzed mainly by cytochrome P450 reductase, several reactive metabolites including nitroso and *N*-hydroxylamine derivatives could be produced. The reductive metabolite of tacrine is produced by cytochrome P450 reductase in HepG2 cells, and the enhanced reactive oxygen species production results in cytotoxic effects (Osseni et al., 1999). Cytochrome P450 reductase is also involved in nitrofurantoin-induced redox cycling and cytotoxicity (Wang et al., 2008). There is no report suggesting the involvement of CYP3A4 in the metabolic activation of tacrine and nitrofurantoin. From these lines of evidence, the positive cytotoxic effects of tacrine and nitrofurantoin in Fig. 2 would be due to the cytochrome P450 reductase activity, which is highly expressed in tumor cells compared with hepatocytes. Flutamide is known to induce severe hepatic dysfunction. Ohbuchi et al. (2009) suggested that CYP3A4 catalyzed the N-oxidation of the amino metabolite of flutamide, which had hepatotoxic effects. Dantrolene was also implicated in the generation of reactive oxygen species via cytochrome P450 reductase. However, we previously reported that CYP3A4-mediated cytotoxicity was not involved in the effects of the nitroaromatic drugs, flutamide and dantrolene, which we investigated using CYP3A4-expressing rat BRL3A cells (Yoshikawa et al., 2009), supporting our present data in Fig. 2. Although the cytochrome P450 reductase-mediated redox reactions were suggested in flutamide- and dantrolene-induced hepatotoxicities, the underlying mechanism for metabolic activation is likely to be different for different drugs, producing different cytotoxic outcomes, an issue that needs to be clarified.

Felbamate induces the activity of CYP3A4, which accounts for the in vivo drug interactions in human (Glue et al., 1997). It was reported that felbamate heteroactivates the CYP3A4-mediated pathway (Egnell et al., 2003). However, these kinds of adverse effects were not detected in the present assay system, because only the cytotoxic effect by the CYP3A4-mediated metabolic activation of drug could be assessed. In addition, hepatotoxicity and hypersensitivity syndromes are associated with allopurinol (Al-Kawas et al., 1981; Arellano and Sacristán, 1993). Although the involvement of the CYP3A4-mediated reaction was still not clear, this kind of hepatotoxicity was also not detected in the present system.

A cytotoxic effect of metabolic activation of drug by CYP3A4 (Fig. 2, ●) was clearly demonstrated in a dose-dependent manner at 10 and 25 μM desipramine and nitrofurantoin. The cytotoxicity of parent drugs was demonstrated to be potent at 50 μM desipramine and nitrofurantoin and amiodarone (Fig. 2, ●). Thus, the effect of metabolic activation by CYP3A4 could not be detected at 50 μM concentrations of the drugs (Fig. 2), indicating that it should be considered the cytotoxicity of active metabolite(s) as well as that of the parent drugs at the various concentrations of drugs used in this in vitro assay system.

Nrf2 is the main regulator of the up-regulation of genes associated with detoxification reactions and is known to be constitutively and ubiquitously expressed in several tissues and cell lines. In the absence